



AD-A279 100



ESL-TR-89-01

(2)

AIRCRAFT TIRE/PAVEMENT PRESSURE DISTRIBUTION

J.T. TIELKING

TEXAS A&M UNIVERSITY
TEXAS TRANSPORTATION INSTITUTE
TEXAS A&M UNIVERSITY
COLLEGE STATION TX 77843

JUNE 1989

FINAL REPORT

JULY 1988 — JANUARY 1989

DTIC
SELECTED
MAY 11 1994
S B D

APPROVED FOR PUBLIC RELEASE:
DISTRIBUTION UNLIMITED

94-13972



AIR FORCE ENGINEERING & SERVICES CENTER
ENGINEERING & SERVICES LABORATORY
TYNDALL AIR FORCE BASE, FLORIDA 32403

DTIC QUALITY ASSURED 1
94 5 09 063

NOTICE

PLEASE DO NOT REQUEST COPIES OF THIS REPORT FROM
HQ AFESC/RD (ENGINEERING AND SERVICES LABORATORY).
ADDITIONAL COPIES MAY BE PURCHASED FROM:

NATIONAL TECHNICAL INFORMATION SERVICE
5285 PORT ROYAL ROAD
SPRINGFIELD, VIRGINIA 22161

FEDERAL GOVERNMENT AGENCIES AND THEIR CONTRACTORS
REGISTERED WITH DEFENSE TECHNICAL INFORMATION CENTER
SHOULD DIRECT REQUESTS FOR COPIES OF THIS REPORT TO:

DEFENSE TECHNICAL INFORMATION CENTER
CAMERON STATION
ALEXANDRIA, VIRGINIA 22314

UNCLASSIFIED

Form Approved
OMB No. 0704-0188

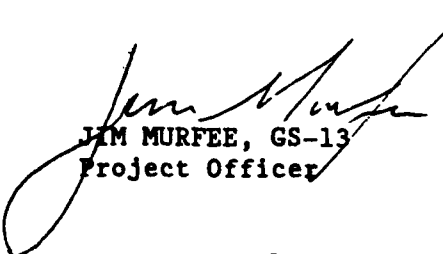
PREFACE

This report was prepared by the Texas Transportation Institute of Texas A&M University, funded under Contract Number F08635-88-C-0241 by the Air Force Civil Engineering Support Agency, Civil Engineering Laboratory, Tyndall Air Force Base, Florida 32403-5319.

This report covers work performed between 1 July 1988 and 31 January 1989. The AFCESA/RD project officer was Jim Murfee.

This report has been reviewed by the Public Affairs Office and is releasable to the National Technical Information Service (NTIS). At NTIS, it will be available to the general public, including foreign nationals.

This technical report has been reviewed and is approved for publication.



JIM MURFEE, GS-13
Project Officer



FELIX T. UHLIK III, Lt Col, USAF
Chief, Air Base Systems Branch



EDGAR F. ALEXANDER, GM-14
Chief, Air Base Operability and
Repair Section

| | |
|--------------------|-------------------------------------|
| Accession For | |
| NTIS GRA&I | <input checked="" type="checkbox"/> |
| DTIC TAB | <input type="checkbox"/> |
| Unrestricted | <input type="checkbox"/> |
| Jus ad Bellum | <input type="checkbox"/> |
| By _____ | |
| Distribution/ | |
| Availability Order | |
| Dist | Avail And/or Special |
| 1 | - |

TABLE OF CONTENTS

| Section | Title | Page |
|----------|---|------|
| I | INTRODUCTION | 1 |
| | A. OBJECTIVE | 1 |
| | B. BACKGROUND | 1 |
| | C. SCOPE/APPROACH | 2 |
| II | CALCULATED RESULTS | 4 |
| | A. PRESSURE DISTRIBUTIONS | 4 |
| | B. DEFLECTION-LOAD PLOTS | 4 |
| | C. TABULAR DATA | 12 |
| | D. EFFECT OF INFLATION PRESSURE AND TIRE LOAD | 36 |
| III | CONCLUSIONS AND RECOMMENDATIONS | 41 |
| | A. CONCLUSIONS | 41 |
| | B. RECOMMENDATIONS | 42 |
| | REFERENCES | 43 |
| APPENDIX | | |
| A | TIRE DATA AND PROFILES | 45 |

LIST OF FIGURES

| Figure | Title | Page |
|--------|--|------|
| 1 | Pavement Pressure Distribution Produced by a 20x4.4 (T-38) Tire at Rated Inflation Pressure and Load | 5 |
| 2 | Pavement Pressure Distribution Produced by a 25.5x8.0-14 (F-16) Tire at Rated Inflation Pressure and Load | 6 |
| 3 | Pavement Pressure Distribution Produced by a 30x11.5-14.5 (F-4C/G) Tire at Rated Inflation Pressure and Load | 7 |
| 4 | Pavement Pressure Distribution Produced by a 36x11R18 (F-15E) Tire at Rated Inflation Pressure and Load | 8 |
| 5 | Pavement Pressure Distribution Produced by a 49x17 (C-5B) Tire at Rated Inflation Pressure and Load | 9 |
| 6 | Pavement Pressure Distribution Produced by a 20.00-20 (C-130E) Tire at Rated Inflation Pressure and Load | 10 |
| 7 | Pavement Pressure Distribution Produced by a B46x16.0-23.5 (B-1B) Tire at Rated Inflation Pressure | 11 |
| 8 | Comparison of Calculated with Measured Deflection-Load Data for 20x4.4 (T-38) Tire at Rated Inflation Pressure | 13 |
| 9 | Comparison of Calculated with Measured Deflection-Load Data for 25.5x8.0-14 (F-16) Tire at Rated Inflation Pressure | 14 |
| 10 | Comparison of Calculated with Measured Deflection-Load Data for 30x11.5-14.5 (F-4C/G) Tire at Rated Inflation Pressure ... | 15 |
| 11 | Comparison of Calculated with Measured Deflection-Load Data for 36x11R18 (F-15E) Tire at Rated Inflation Pressure | 16 |
| 12 | Comparison of Calculated with Measured Deflection-Load Data for 49x17 (C-5B) Tire at Rated Inflation Pressure | 17 |
| 13 | Comparison of Calculated with Measured Deflection-Load Data for 20.00-20 (C-130E) Tire at Rated Inflation Pressure | 18 |
| 14 | Comparison of Calculated with Measured Deflection-Load Data for B46x16.0-23.5 (B-1B) Tire at Rated Inflation Pressure | 19 |
| 15 | Calculated Pressure Locations in Footprint of T-38 Tire, Full-Scale | 29 |
| 16 | Calculated Pressure Locations in Footprint of F-16 Tire, Half-Scale | 30 |

LIST OF FIGURES
(CONCLUDED)

| Figure | Title | Page |
|--------|--|------|
| 17 | Calculated Pressure Locations in Footprint of F-4C/G Tire, Half-Scale | 31 |
| 18 | Calculated Pressure Locations in Footprint of F-15E Tire, Half-Scale | 32 |
| 19 | Calculated Pressure Locations in Footprint of C-5B Tire, Half-Scale | 33 |
| 20 | Calculated Pressure Locations in Footprint of C-130E Tire, Quarter-Scale | 34 |
| 21 | Calculated Pressure Locations in Footprint of B-1B Tire, Half-Scale | 35 |
| 22 | Pavement Pressure Distribution Produced by the F-4C/G Tire at Rated Inflation Pressure and 25 Percent Overload | 37 |
| 23 | Pavement Pressure Distribution Produced by the F-4C/G Tire at Rated Inflation Pressure and 25 Percent Underload | 38 |
| 24 | Pavement Pressure Distribution Produced by the F-4C/G Tire at 15 Percent Overpressure and Rated Load | 39 |
| 25 | Pavement Pressure Distribution Produced by the F-4C/G Tire at 15 Percent Underpressure and Rated Load | 40 |
| A-1 | Meridian Sections of (a) 25.5x8.0-14 (F-16), (b) 20x4.4 (T-38), Both Full Size | 49 |
| A-2 | Meridian Section of 30x11.5-14.5 (F-4C/G), Full Size | 51 |
| A-3 | Meridian Section of 36x11R18 (F-15E), Full Size | 53 |
| A-4 | Meridian Section of 49x17 (C-5B), Reduced 64 Percent | 55 |
| A-5 | Meridian Section of 20.00-20 (C-130), Reduced 50 Percent | 57 |
| A-6 | Meridian Section of B46x16.0-23.5 (B-1B), Reduced 64 Percent.. | 59 |

LIST OF TABLES

| Table | Title | Page |
|-------|--|------|
| 1 | TIRES STUDIED, RATED INFLATION PRESSURE AND LOAD, FOOTPRINT AREA | 3 |
| 2 | CONTACT PRESSURES, p , IN FOOTPRINT OF 20X4.4 (T-38) TIRE WITH 265 PSI INFLATION PRESSURE AND 6,000 POUND LOAD | 20 |
| 3 | CONTACT PRESSURES, p , IN FOOTPRINT OF 25.5X8.0-14 (F16) TIRE WITH 310 PSI INFLATION PRESSURE AND 16,200 POUND LOAD | 21 |
| 4 | CONTACT PRESSURES, p , IN FOOTPRINT OF 30X11.5-14.5 (F-4C/G) TIRE WITH 265 PSI INFLATION PRESSURE AND 26,000 POUND LOAD.. | 22 |
| 5 | CONTACT PRESSURES, p , IN FOOTPRINT OF 36X11R18 (F15E) TIRE WITH 305 PSI INFLATION PRESSURE AND 35,700 POUND LOAD | 23 |
| 6 | CONTACT PRESSURES, p , IN FOOTPRINT OF 49X17 (C-5B) TIRE WITH 170 PSI INFLATION PRESSURE AND 39,600 POUND LOAD | 24 |
| 7 | CONTACT PRESSURES, p , IN FOOTPRINT OF 20.00-20 (C-130E) TIRE WITH 125 PSI INFLATION PRESSURE AND 46,500 POUND LOAD | 25 |
| 8 | CONTACT PRESSURES, p , IN FOOTPRINT OF B46X16.0-23.5 (B-1B) TIRE WITH 260 PSI INFLATION PRESSURE AND 53,800 POUND LOAD ... | 27 |

SECTION I

INTRODUCTION

A. OBJECTIVE

The primary purpose of the work reported here was to determine the pavement pressure distribution produced by a variety of aircraft tires used by the Air Force. The tire/pavement pressure distributions are needed by airfield pavement engineers concerned with the design of thin flexible pavements for aircraft using high pressure tires to carry heavy loads.

B. BACKGROUND

Pavement design has traditionally been based on the assumptions that a tire's footprint is circular and exerts a uniform pressure on the pavement surface. The magnitude of the pressure is often taken as equal to the inflation pressure although other values have been specified which are related to the expected footprint area (Reference 1). Although the assumption of uniform tire/pavement contact pressure has led to successful airfield pavement design for many years, modern aircraft with high-pressure tires to carry heavy loads are creating new demands for pavement performance.

Modern pavement models, based on the finite element method, can account for nonuniformity in the surface pressure produced by a tire. It has been established that, for a truck tire, the shape of the tire/pavement pressure distribution has a significant effect on strains in a flexible highway pavement (Reference 2). The actual shape of the aircraft tire/pavement pressure distribution is thus, becoming of considerable interest to airfield pavement engineers.

In view of the lack of measurement of aircraft tire/pavement pressure distributions, and the expense of making such measurements, the present project was initiated to calculate representative pressure distributions using a computer tire model.

C. SCOPE/APPROACH

As few previous studies of aircraft tire/pavement pressure distributions exist, the project was begun by developing a list of tires that would include a wide range of tire sizes, inflation pressures, and tire loads. This list is given in Table 1, and the tires are arranged according to their rated loads. All of the tires are main gear tires, for the aircraft identified in Table 1. Only one radial tire (for the F-15E airplane) is included in the study as virtually all aircraft tires today are of conventional bias-ply design. The relative sizes of the tires can be seen by turning to Appendix A where meridian profile plots are shown.

The tire/pavement pressure distributions were made with a finite element tire model developed previously at Texas A&M University (Reference 3). This model utilizes a relatively comprehensive description of a tire's geometry and material properties, without requiring an excessive amount of computer time. Most of the calculations were made with a VAXstation 2000 workstation-class computer. The 3-D plots shown in the next section were made with the SAS graphics package on a mainframe computer.

Input data describing a tire to the tire model were obtained from various sources, including the tire Qualification Test Report (QTR), the tire manufacturer, and a physical section of the tire. Tire sections for this project were provided by Mr. Jack Passey and Mr. Brian Chatterton of Hill AFB, Utah; Mr. Bob Fitzharris of Wright-Patterson AFB, Ohio; and Mr. H.G. Herchenroether of B.F. Goodrich Aerospace and Defense. A detailed description of the input data needed by the tire model is given in Appendix A.

TABLE 1. TIRES STUDIED, RATED INFLATION PRESSURE AND LOAD, FOOTPRINT AREA.

| Airplane | Tire Size | Pressure (psi) | Load (lb) | Area (in. ²) | Tire Mfr. | QTR No. |
|----------|-----------------------------|----------------|-----------|--------------------------|-----------|--------------|
| T-38 | 20x4.4/14 | 265 | 6,000 | 24.4 | Goodrich | 72037-1-TL |
| F-16 | 25.5x8.0-14/20 | 310 | 16,200 | 53.0 | Goodrich | 83011-2-TL |
| F-4C/G | 30x11.5-14.5/z ₀ | 265 | 26,600 | 105.0 | Goodyear | 461B-3119-TL |
| F-15E | 36x11R18 | 305 | 35,800 | 119.8 | Michelin | M03803 |
| C-5B | 49x17/26 | 170 | 39,600 | 231.0 | Goodrich | 72027-2-TL |
| C-130E | 20.00-20/26 | 125 | 46,500 | 445.7 | Goodrich | 32004-3-TL |
| B-1B | B46x16.0-23.5/30 | 260 | 53,800 | 209.0 | Goodrich | 83010-1-TL |

SECTION II

CALCULATED RESULTS

The tire model that provided the calculated results given here represents the tire as a layered toroidal shell of revolution. Cord and rubber properties of each cord-reinforced layer are specified separately. The tread layer (rubber only) is not included in the model. Tire inflation pressure is input to the model and the inflated shape of the tire is calculated. The model is then deflected against a flat, frictionless surface and the contact pressure distribution is calculated. This contact pressure distribution is approximately what would be produced by a tire without a tread, standing on a smooth surface. It is believed to exhibit the essential features of the pavement pressure in the footprint of an actual tire, at the same inflation pressure and tire load.

A. PRESSURE DISTRIBUTIONS

Figures 1-7 show 3-D plots of pavement pressure distributions calculated for the seven tires listed in Table 1. These distributions represent the normal contact pressure applied to the pavement by each tire (standing condition) at its rated inflation pressure and rated load. In these figures, x indicates the direction of tire travel and y is directed across the tread. The normalized contact pressure (NCP) shown in the figures is obtained by dividing the calculated contact pressure, p, by the rated inflation pressure for the tire. The calculated pressure values are given in tables in Part C of this section.

B. DEFLECTION-LOAD PLOTS

The integral, or resultant, of the pavement pressure distribution gives the tire load. Since the tire model used in this work is a deflection-

Normalized contact pressure - T-38 tire
(6000 LB LOAD, 265 PSI INFLATION)
(NORMALIZED TO INFLATION PRESSURE)

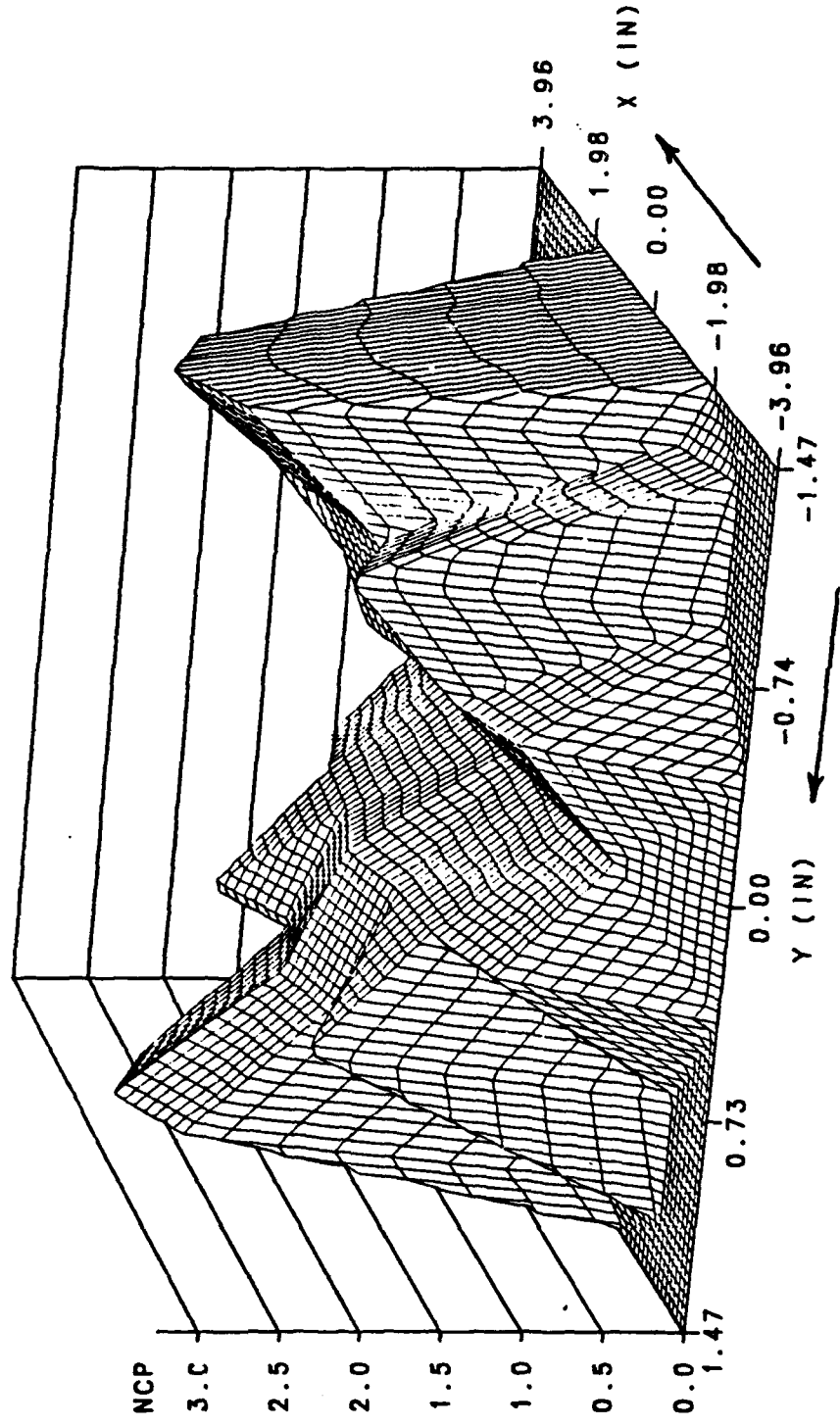


Figure 1. Pavement Pressure Distribution Produced by a 20x4.4
(T-38) Tire at Rated Inflation Pressure and Load.

Normalized contact pressure - F-16 tire
(16200 LB LOAD, 310 PSI INFLATION)
(NORMALIZED TO INFLATION PRESSURE)

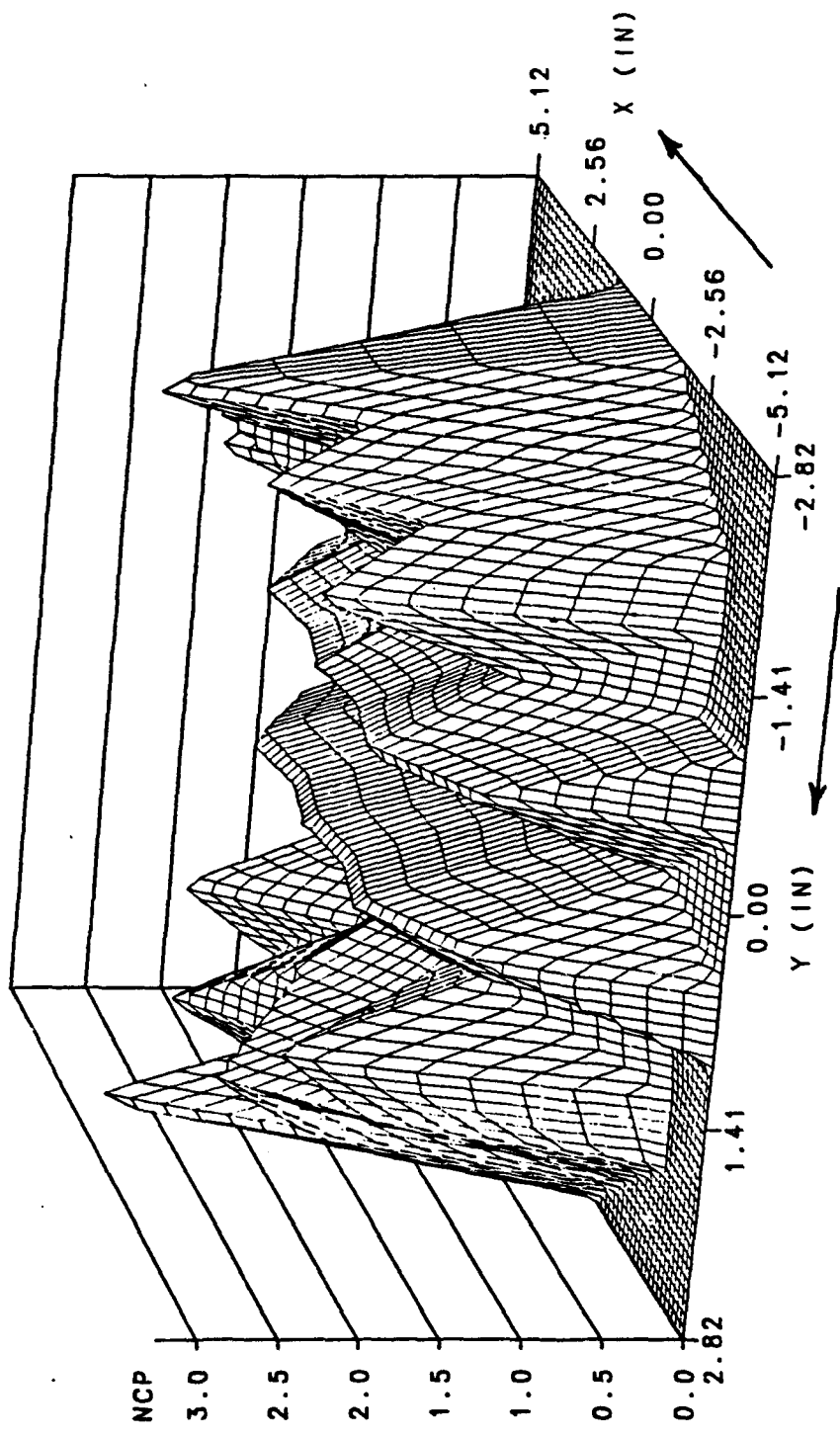


Figure 2. Pavement Pressure Distribution Produced by a 25.5x8.0-14
(F-16) Tire at Rated Inflation Pressure and Load.

Normalized contact pressure - F-4 tire
(2660 LB LOAD, 265 PSI INFLATION)
(NORMALIZED TO INFLATION PRESSURE)

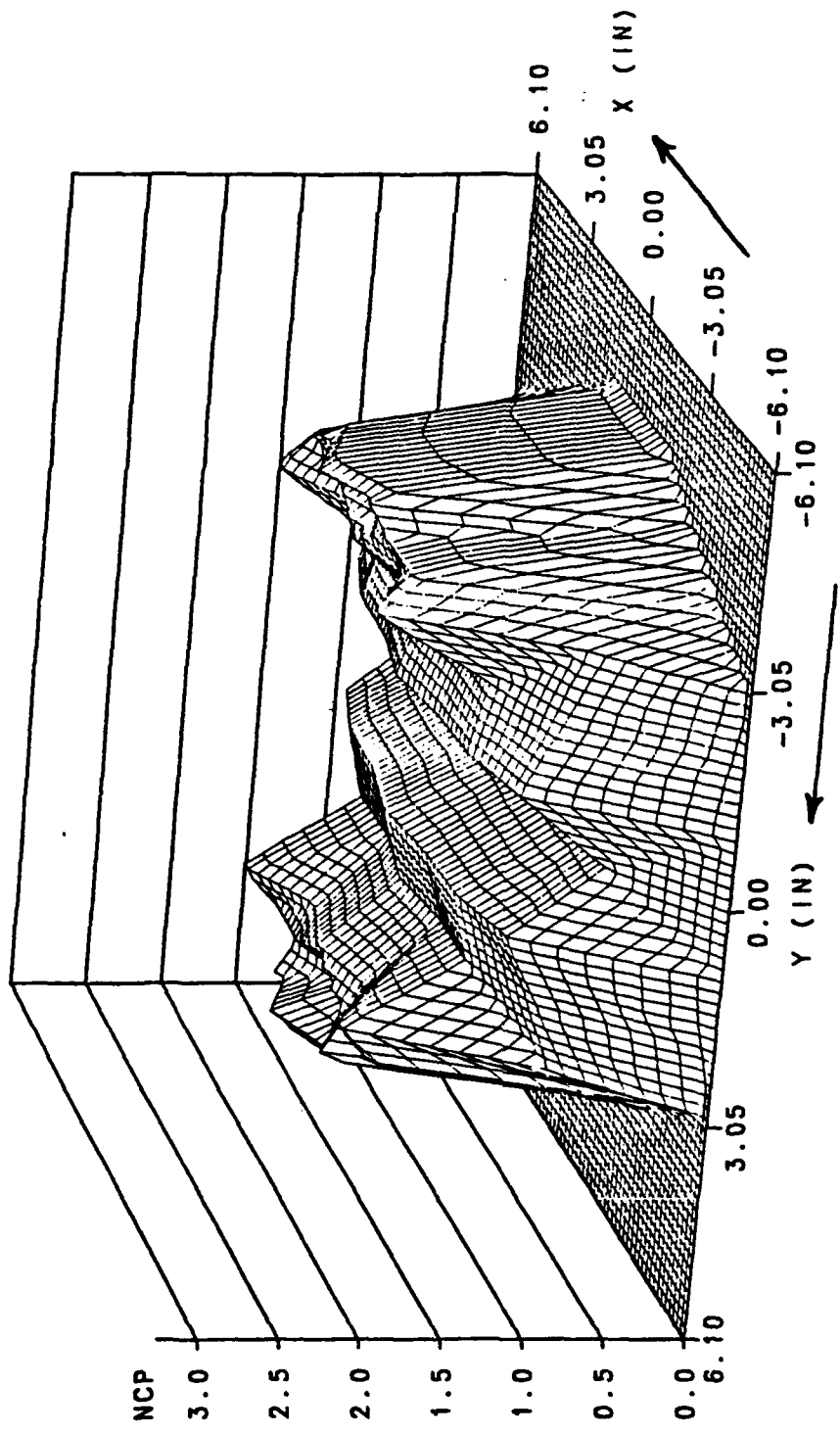


Figure 3. Pavement Pressure Distribution Produced by a 30x11.5-14.5 (F-4C/G) Tire at Rated Inflation Pressure and Load.

Normalized contact pressure - F-15E tire
(3500 LB LOAD, 305 PSI INFLATION)
(NORMALIZED TO INFLATION PRESSURE)

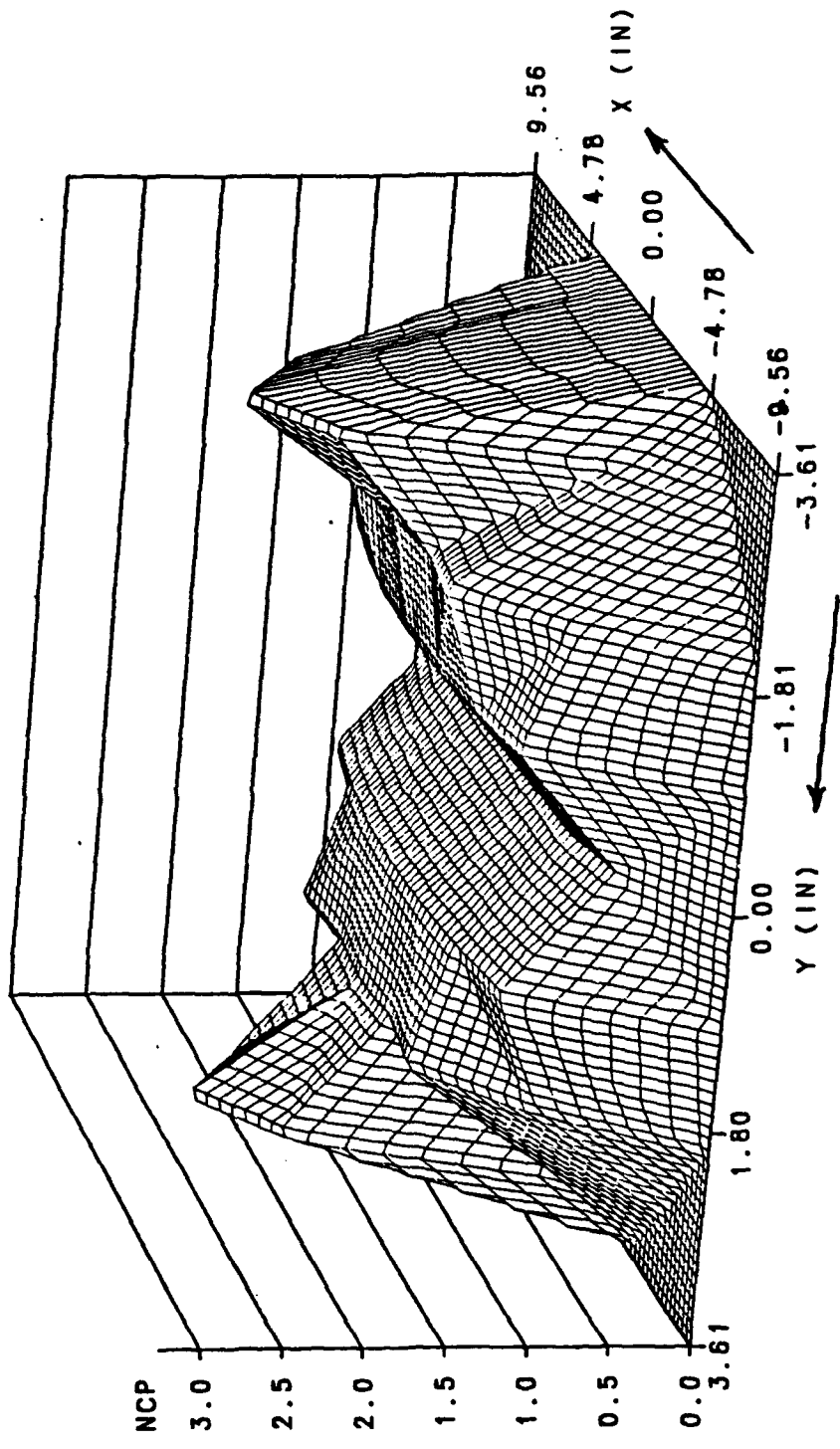


Figure 4. Pavement Pressure Distribution Produced by a 36x11R18 (F-15E) Tire at Rated Inflation Pressure and Load.

Normalized contact pressure - C-5B tire
(39600 LB LOAD, 170 PSI INFLATION)
(NORMALIZED TO INFLATION PRESSURE)

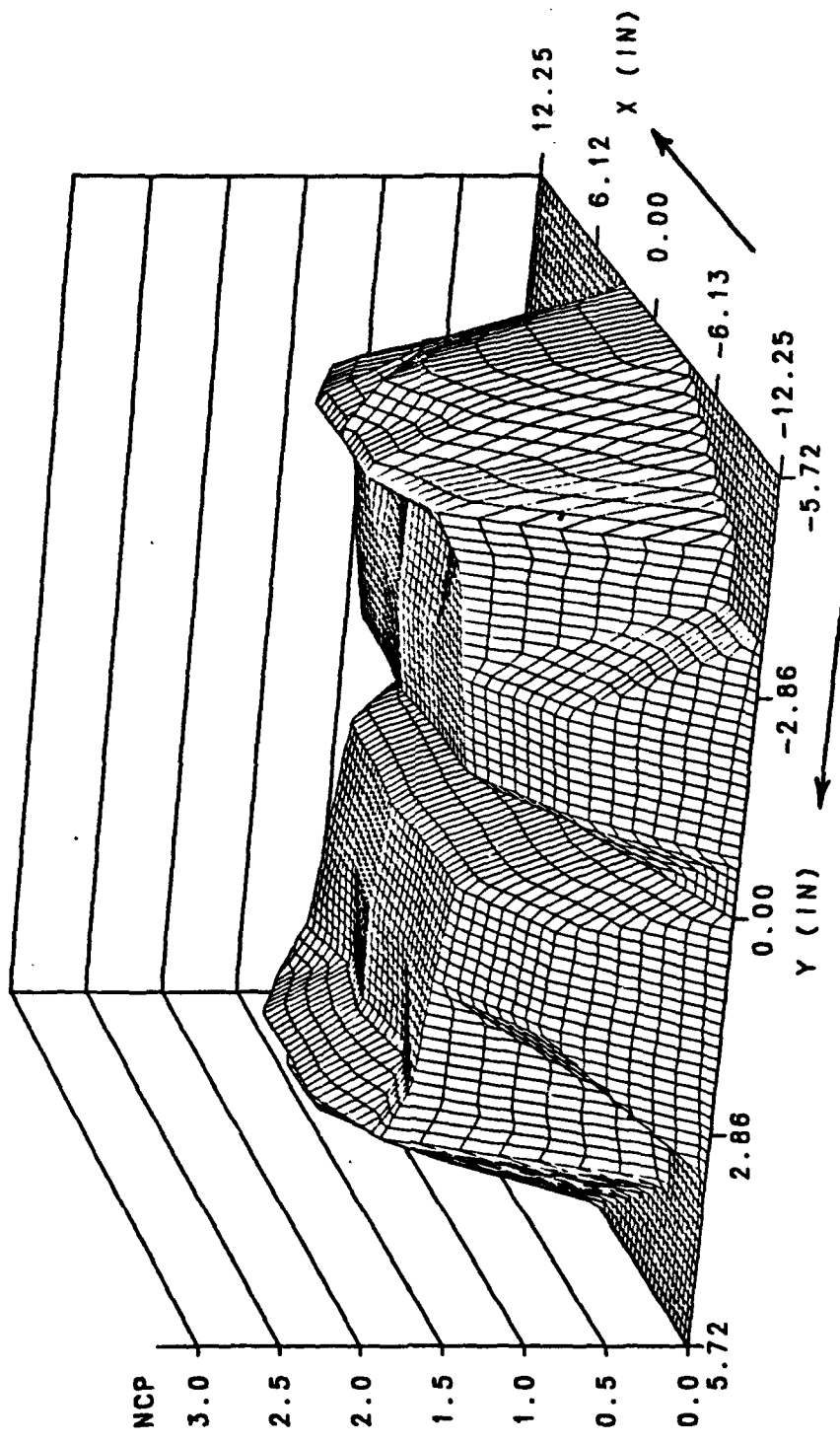


Figure 5. Pavement Pressure Distribution Produced by a 49x17
(C-5B) Tire at Rated Inflation Pressure and Load.

Normalized contact pressure - C-130 tire
125 psi inflation pressure
46500 lb load, normalized to
(46500 lb load, normalized to)

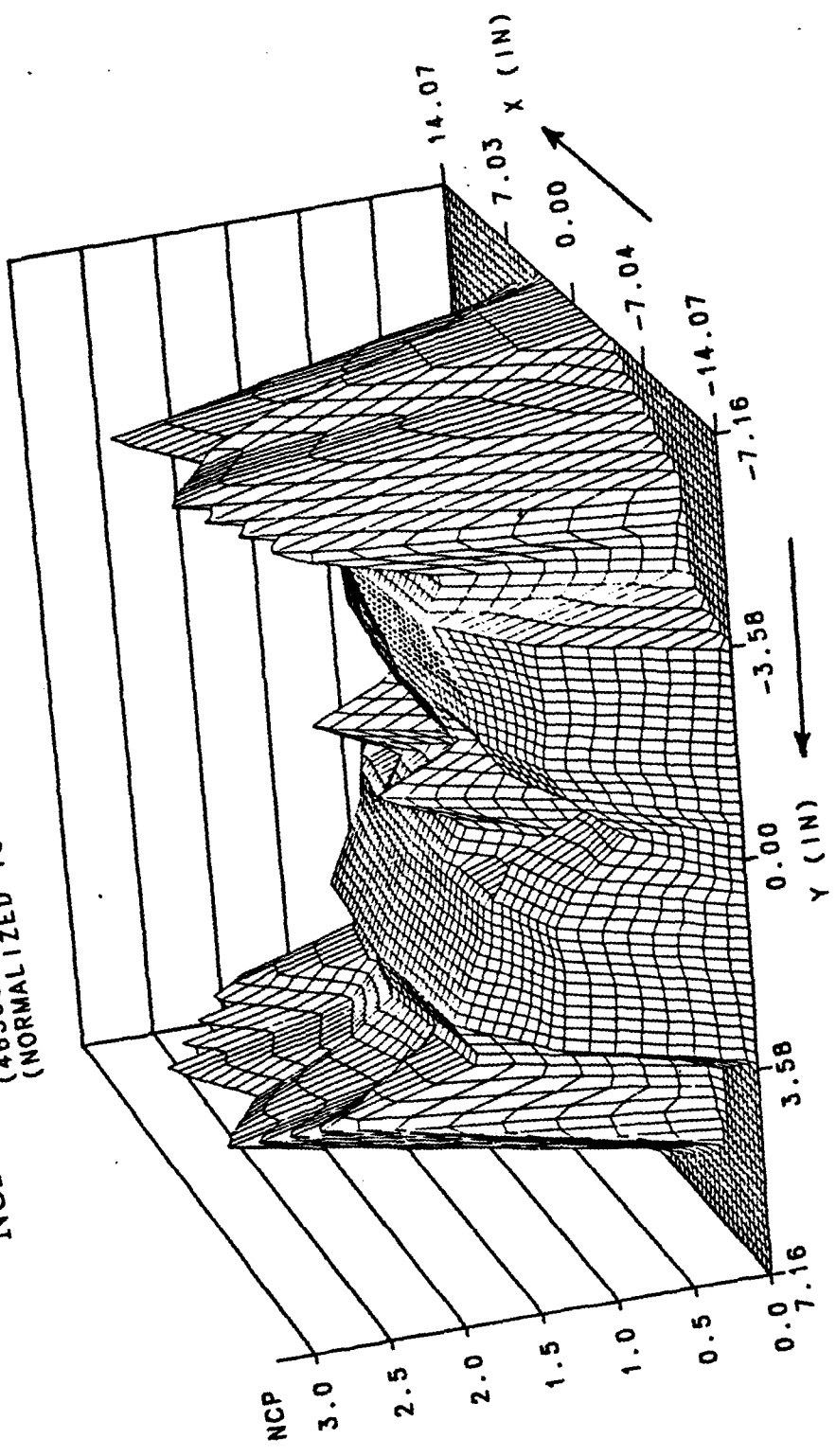


Figure 6. Pavement pressure distribution produced by a 20.00-20
(C-130) Tire at Rated Inflation Pressure and Load.

Normalized contact pressure - B-1B tire
(53800 LB LOAD, 260 PSI INFLATION)
(NORMALIZED TO INFLATION PRESSURE)

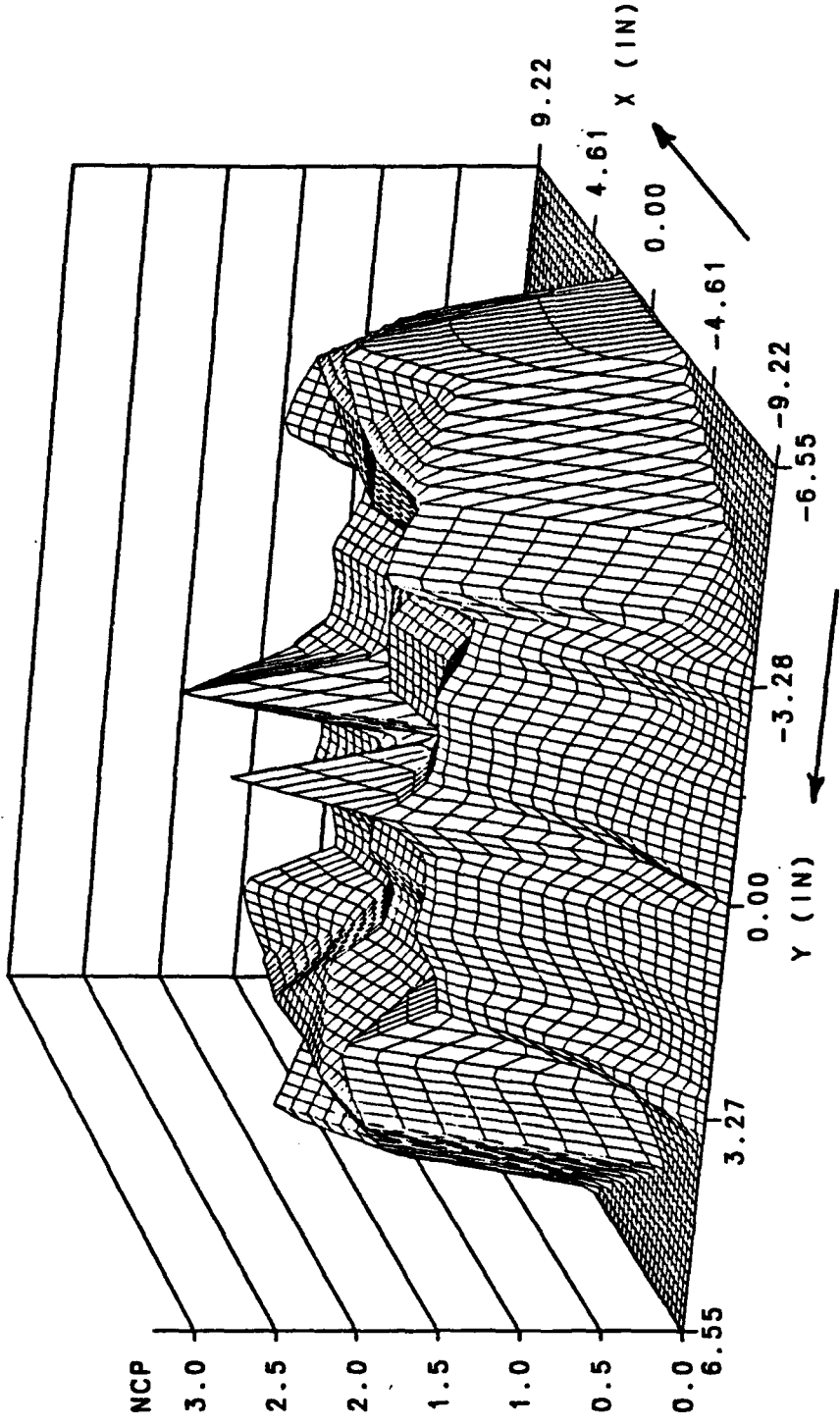


Figure 7. Pavement Pressure Distribution Produced by a B46x16.0-23.5
(B-1B) Tire at Rated Inflation Pressure and Load.

specified model*, comparing the calculated tire load with the load measured at the same tire deflection indicates validity of the tire model.

Figures 8-14 show a comparison of measured deflection-load data, taken from the tire QTR, with calculated deflection-load data for each tire at its rated inflation pressure. The comparison is fairly good in the neighborhood of each tire's rated load. In all cases, however, the slope of the calculated data is less than the slope of the measured data. This indicates that the tire model is somewhat stiffer than the tire being modeled. Consequently, the calculated pavement pressures may be more nonuniform than the actual pavement pressures.

C. TABULAR DATA

Tables 2-8 give the locations and numerical values of contact pressure, p , calculated in the footprint of each tire at rated inflation pressure and rated load. As the tire model footprint has two axes of symmetry, contact pressures in one quarter of the footprint are calculated. The location of each point where a pressure is found is given by Cartesian coordinates, x and y , which originate at the center of the footprint. For example, Figure 15 shows the complete set of points where contact pressures are obtained for the 20x4.4 (T-38) tire. The tire model calculates pressures at points 1 through 21 (Table 2 and Figure 15) for the T-38 tire. The pressures at the unnumbered points in Figure 15 are identified by reflection across the footprint axes of symmetry (the x and y axes). The footprint locations of contact pressures for the other tires (Tables 3-8 and Figures 16-21) are similarly determined. The

*With this model, a tire deflection is specified as input data and the consequent load is obtained by integrating the calculated contact pressure distribution.

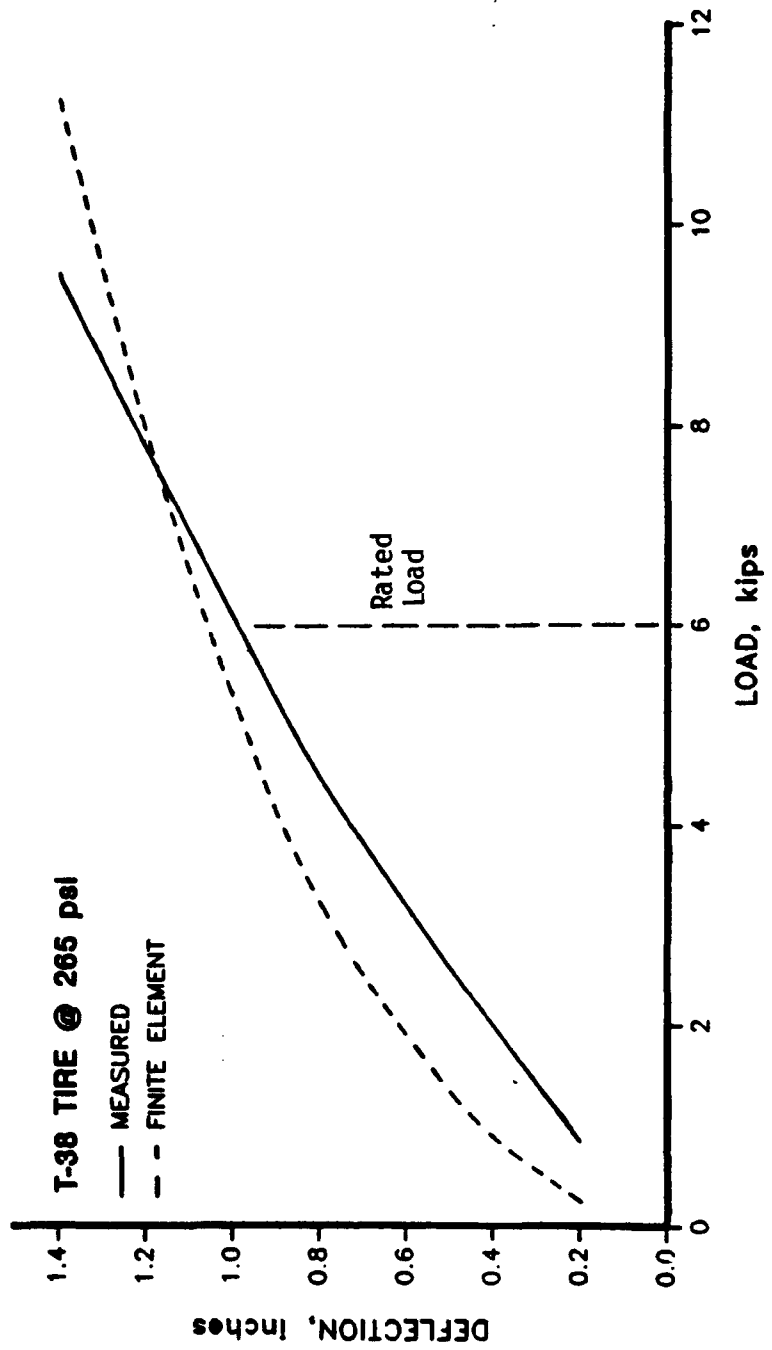


Figure 8. Comparison of Calculated with Measured Deflection-Load Data for 20x4.4 (T-38) Tire at Rated Inflation Pressure.

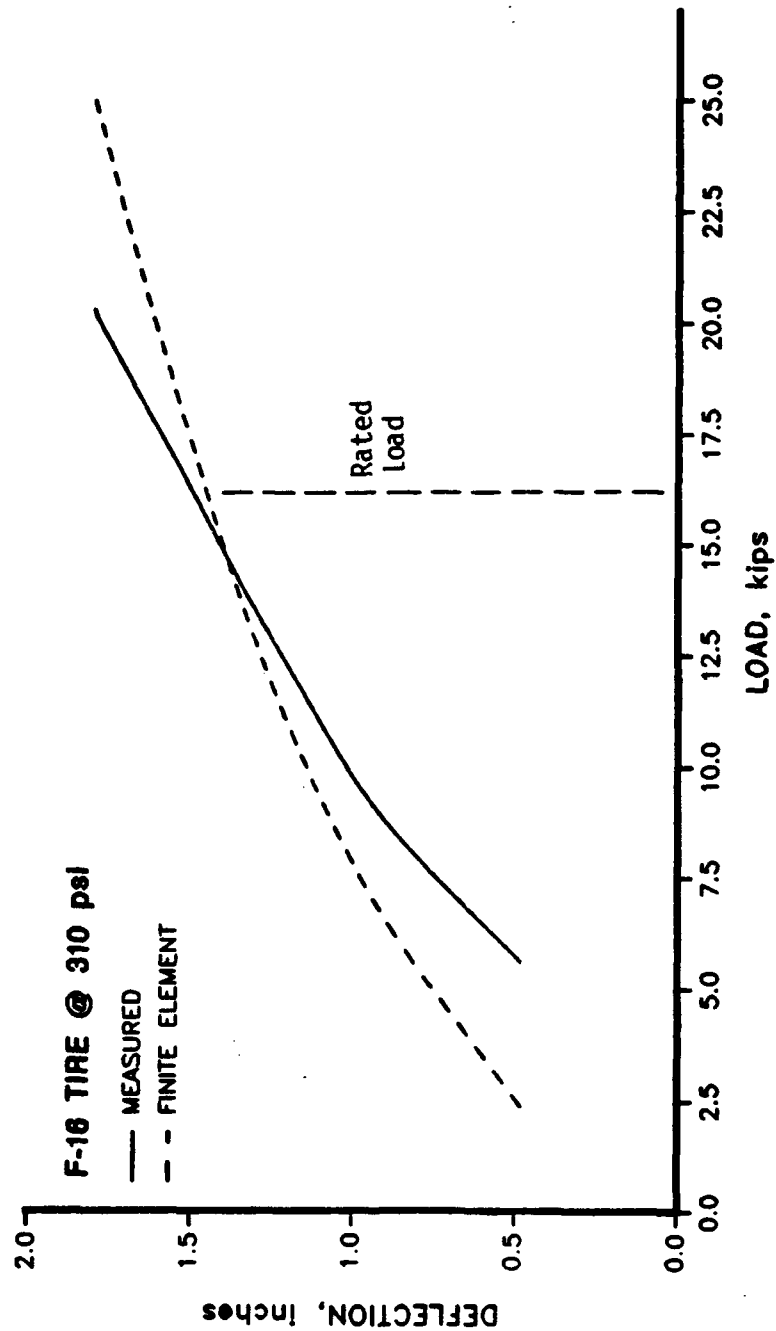


Figure 9. Comparison of Calculated with Measured Deflection-Load Data for 25.5x8.0-14 (F-16) Tire at Rated Inflation Pressure.

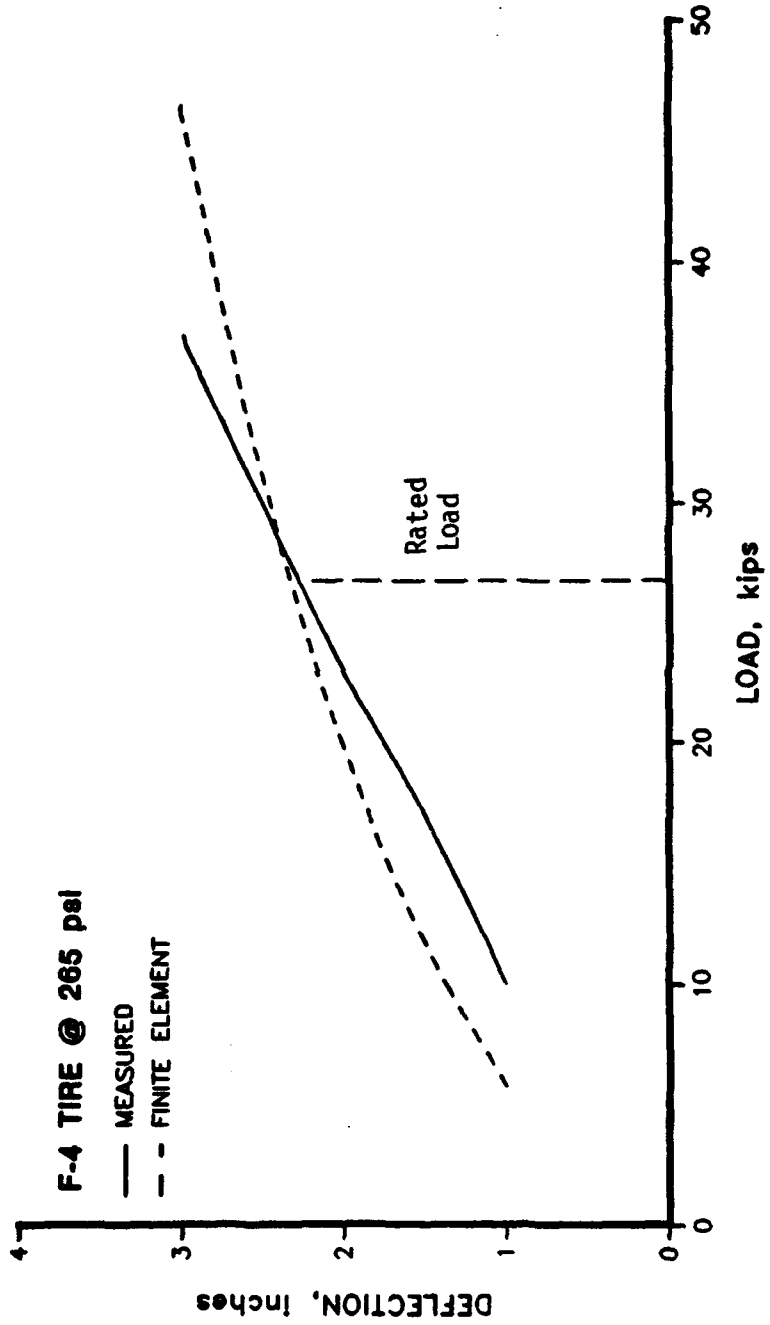


Figure 10. Comparison of Calculated with Measured Deflection-Load Data for 30x11.5-14.5 (F-4C/G) Tire at Rated Inflation Pressure.

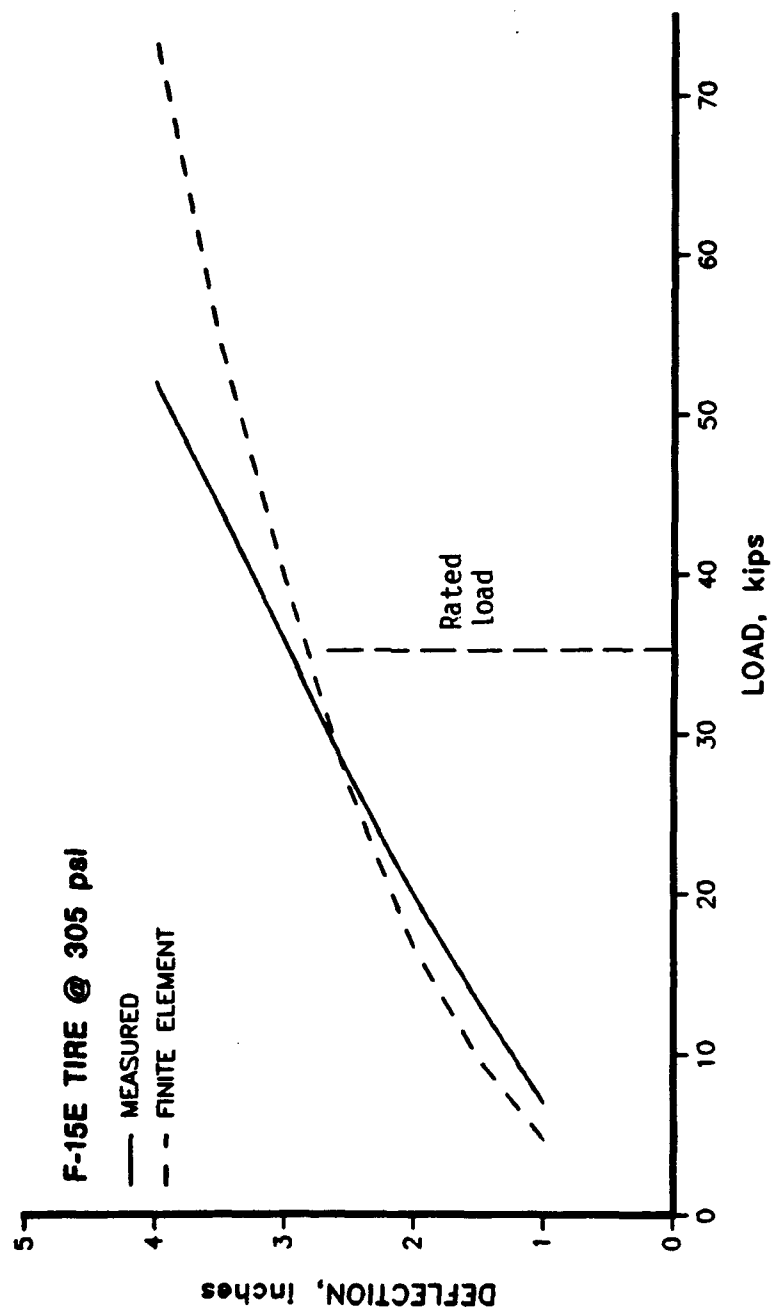


Figure 11. Comparison of Calculated with Measured Deflection-Load Data for 36x11R18 (F-15E) Tire at Rated Inflation Pressure.

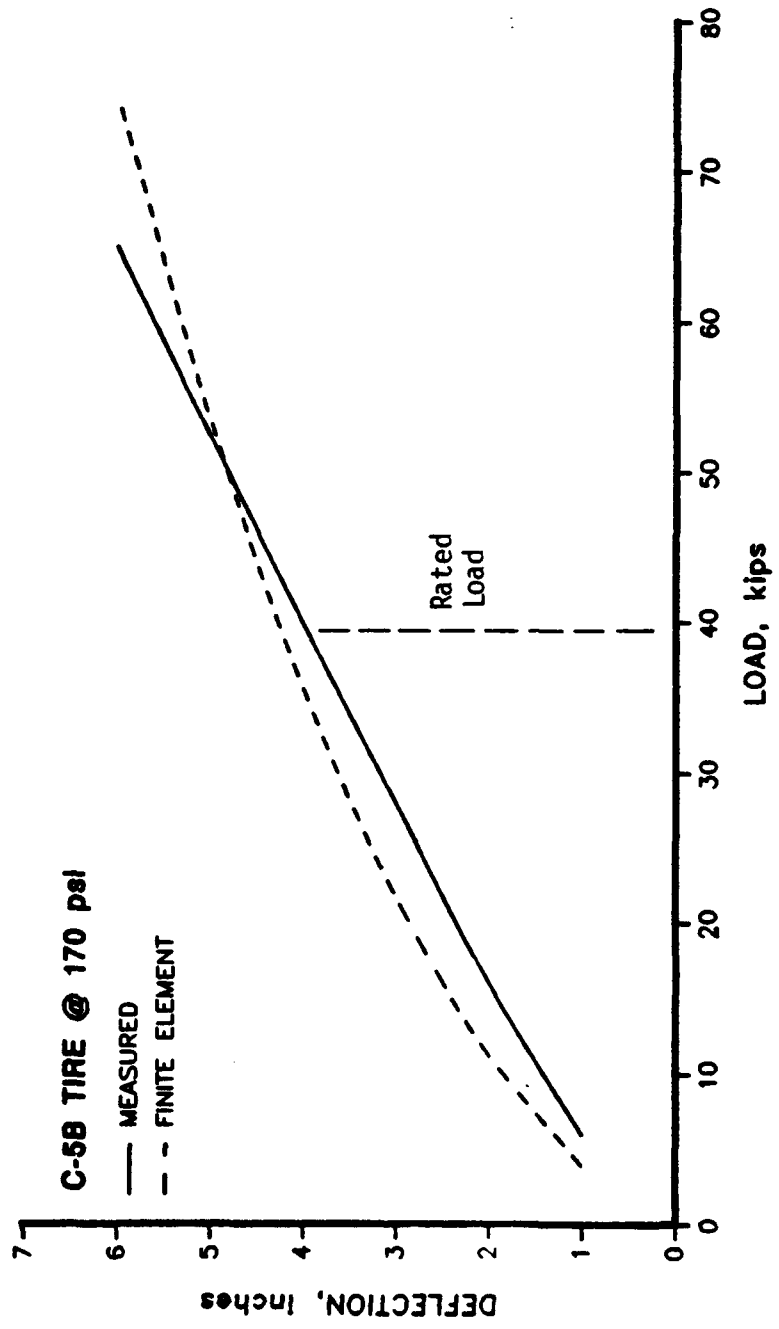


Figure 12. Comparison of Calculated with Measured Deflection-Load Data for 49x17 (C-5B) Tire at Rated Inflation Pressure.

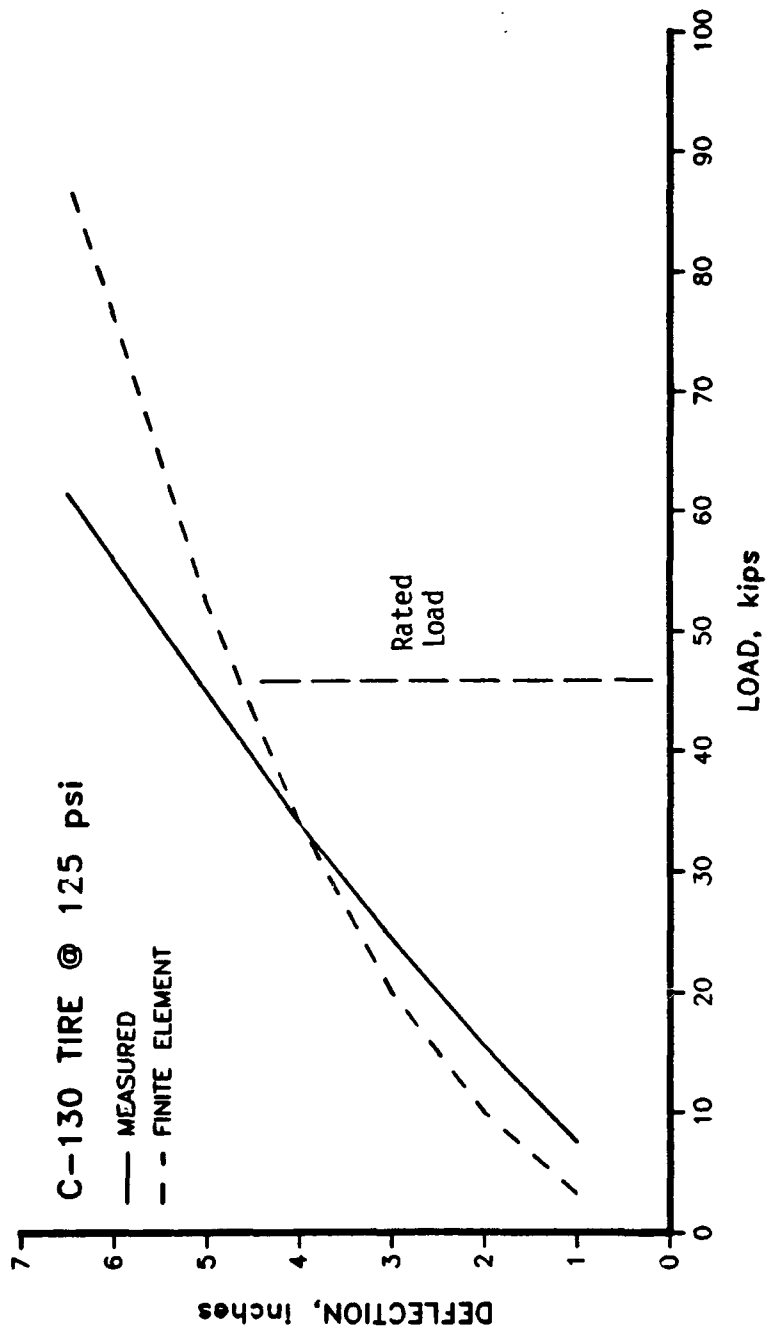


Figure 13. Comparison of Calculated with Measured Deflection-Load Data for C.J.00-20 (C-130) Tire at Rated Inflation Pressure.

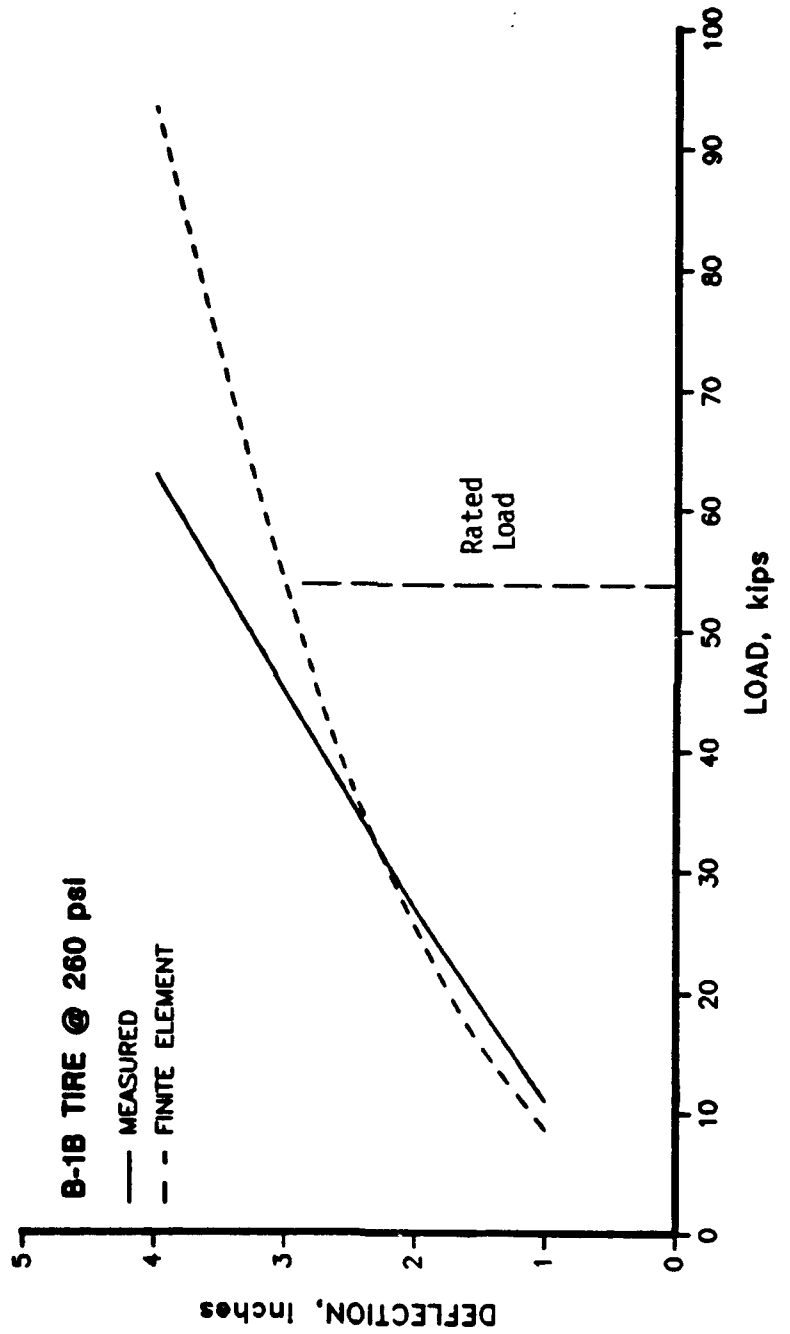


Figure 14. Comparison of Calculated with Measured Deflection-Load Data for B46x16.0-23.5 (B-1B) Tire at Rated Inflation Pressure.

TABLE 2. CONTACT PRESSURES, p , IN FOOTPRINT OF 20x4.4 (T-38) TIRE
WITH 265 PSI INFLATION PRESSURE AND 6,000 POUND LOAD.

| Point | x (in) | y (in) | p (psi) | NCP |
|-------|--------|--------|-----------|------|
| 1 | 0.0 | 0.0 | 134.4 | 0.51 |
| 2 | 0.99 | 0.0 | 146.5 | 0.55 |
| 3 | 1.98 | 0.0 | 160.1 | 0.60 |
| 4 | 2.97 | 0.0 | 135.9 | 0.51 |
| 5 | 3.96 | 0.0 | 0.0 | 0.0 |
| 6 | 0.0 | 0.40 | 426.9 | 1.61 |
| 7 | 0.98 | 0.40 | 383.9 | 1.45 |
| 8 | 1.97 | 0.40 | 370.4 | 1.40 |
| 9 | 2.95 | 0.40 | 314.2 | 1.18 |
| 10 | 3.94 | 0.40 | 0.0 | 0.0 |
| 11 | 0.0 | 0.82 | 512.3 | 1.93 |
| 12 | 0.97 | 0.82 | 468.2 | 1.77 |
| 13 | 1.93 | 0.82 | 559.3 | 2.11 |
| 14 | 2.90 | 0.82 | 0.0 | 0.0 |
| 15 | 0.0 | 1.27 | 787.1 | 2.97 |
| 16 | 0.94 | 1.27 | 700.6 | 2.64 |
| 17 | 1.87 | 1.27 | 46.6 | 0.18 |
| 18 | 2.81 | 1.27 | 0.0 | 0.0 |
| 19 | 0.0 | 1.47 | 0.0 | 0.0 |
| 20 | 0.92 | 1.47 | 0.0 | 0.0 |
| 21 | 1.83 | 1.47 | 0.0 | 0.0 |

TABLE 3. CONTACT PRESSURES, p , IN FOOTPRINT OF 25.5X8.0-14 (F-16) TIRE
WITH 310 PSI INFLATION PRESSURE AND 16,200 POUND LOAD.

| Point | x (in) | y (in) | p (psi) | NCP |
|-------|--------|--------|---------|------|
| 1 | 0.0 | 0.0 | 49.3 | 0.16 |
| 2 | 1.28 | 0.0 | 72.6 | 0.23 |
| 3 | 2.56 | 0.0 | 112.7 | 0.36 |
| 4 | 3.84 | 0.0 | 62.6 | 0.20 |
| 5 | 5.12 | 0.0 | 0.0 | 0.0 |
| 6 | 0.0 | 0.50 | 604.3 | 1.95 |
| 7 | 1.28 | 0.50 | 576.3 | 1.86 |
| 8 | 2.56 | 0.50 | 606.6 | 1.96 |
| 9 | 3.84 | 0.50 | 473.2 | 1.53 |
| 10 | 5.12 | 0.50 | 0.0 | 0.0 |
| 11 | 0.0 | 1.00 | 349.2 | 1.13 |
| 12 | 1.27 | 1.00 | 232.9 | 0.75 |
| 13 | 2.54 | 1.00 | 328.2 | 1.06 |
| 14 | 3.81 | 1.00 | 16.6 | 0.05 |
| 15 | 5.09 | 1.00 | 0.0 | 0.0 |
| 16 | 0.0 | 1.50 | 572.0 | 1.85 |
| 17 | 1.26 | 1.50 | 400.0 | 1.29 |
| 18 | 2.52 | 1.50 | 716.7 | 2.31 |
| 19 | 3.78 | 1.50 | 0.0 | 0.0 |
| 20 | 0.0 | 2.00 | 581.3 | 1.88 |
| 21 | 1.23 | 2.00 | 775.4 | 2.50 |
| 22 | 2.46 | 2.00 | 504.7 | 1.63 |
| 23 | 3.69 | 2.00 | 0.0 | 0.0 |
| 24 | 0.0 | 2.42 | 979.7 | 3.16 |
| 25 | 1.20 | 2.42 | 563.8 | 1.82 |
| 26 | 2.41 | 2.42 | 0.0 | 0.0 |
| 27 | 0.0 | 2.75 | 0.0 | 0.0 |
| 28 | 1.18 | 2.75 | 0.0 | 0.0 |

TABLE 4. CONTACT PRESSURES, p , IN FOOTPRINT OF 30X11.5-14.5 (F-4C/G) TIRE WITH 265 PSI INFLATION PRESSURE AND 26,600 POUND LOAD.

| Point | x (in) | y (in) | p (psi) | NCP |
|-------|--------|--------|---------|------|
| 1 | 0.0 | 0.0 | 141.9 | 0.54 |
| 2 | 1.53 | 0.0 | 149.1 | 0.56 |
| 3 | 3.05 | 0.0 | 146.9 | 0.55 |
| 4 | 4.58 | 0.0 | 149.9 | 0.57 |
| 5 | 6.10 | 0.0 | 0.0 | 0.0 |
| 6 | 0.0 | 1.00 | 367.2 | 1.39 |
| 7 | 1.52 | 1.00 | 344.1 | 1.30 |
| 8 | 3.04 | 1.00 | 338.8 | 1.28 |
| 9 | 4.56 | 1.00 | 298.8 | 1.13 |
| 10 | 6.08 | 1.00 | 0.0 | 0.0 |
| 11 | 0.0 | 2.00 | 328.6 | 1.24 |
| 12 | 1.50 | 2.00 | 305.0 | 1.15 |
| 13 | 3.00 | 2.00 | 307.1 | 1.16 |
| 14 | 4.50 | 2.00 | 241.4 | 0.91 |
| 15 | 5.99 | 2.00 | 0.0 | 0.0 |
| 16 | 0.0 | 3.00 | 462.2 | 1.74 |
| 17 | 1.46 | 3.00 | 423.9 | 1.60 |
| 18 | 2.92 | 3.00 | 512.8 | 1.94 |
| 19 | 4.39 | 3.00 | 197.7 | 0.75 |
| 20 | 5.85 | 3.00 | 0.0 | 0.0 |
| 21 | 0.0 | 3.52 | 387.5 | 1.46 |
| 22 | 1.43 | 3.52 | 451.2 | 1.70 |
| 23 | 2.87 | 3.52 | 451.3 | 1.70 |
| 24 | 4.30 | 3.52 | 0.0 | 0.0 |
| 25 | 0.0 | 4.06 | 558.0 | 2.10 |
| 26 | 1.40 | 4.06 | 490.7 | 1.85 |
| 27 | 2.80 | 4.06 | 0.0 | 0.0 |
| 28 | 0.0 | 4.65 | 0.0 | 0.0 |
| 29 | 1.35 | 4.65 | 0.0 | 0.0 |

TABLE 5. CONTACT PRESSURES, p , IN FOOTPRINT OF 36X11R18 (F-15E) TIRE
WITH 305 PSI INFLATION PRESSURE AND 35,800 POUND LOAD.

| Point | x (in) | y (in) | p (psi) | NCP |
|-------|--------|--------|---------|------|
| 1 | 0.0 | 0.0 | 186.6 | 0.61 |
| 2 | 2.39 | 0.0 | 191.4 | 0.63 |
| 3 | 4.78 | 0.0 | 191.0 | 0.63 |
| 4 | 7.17 | 0.0 | 156.1 | 0.51 |
| 5 | 9.56 | 0.0 | 0.0 | 0.0 |
| 6 | 0.0 | 1.00 | 407.6 | 1.34 |
| 7 | 2.37 | 1.00 | 402.3 | 1.32 |
| 8 | 4.75 | 1.00 | 383.4 | 1.26 |
| 9 | 7.12 | 1.00 | 355.5 | 1.17 |
| 10 | 9.50 | 1.00 | 0.0 | 0.0 |
| 11 | 0.0 | 2.00 | 449.5 | 1.47 |
| 12 | 2.32 | 2.00 | 435.0 | 1.43 |
| 13 | 4.65 | 2.00 | 456.0 | 1.50 |
| 14 | 6.97 | 2.00 | 274.4 | 0.90 |
| 15 | 9.30 | 2.00 | 0.0 | 0.0 |
| 16 | 0.0 | 3.00 | 769.5 | 2.52 |
| 17 | 2.24 | 3.00 | 632.8 | 2.07 |
| 18 | 4.48 | 3.00 | 146.7 | 0.48 |
| 19 | 6.72 | 3.00 | 0.0 | 0.0 |
| 20 | 0.0 | 3.61 | 0.0 | 0.0 |
| 21 | 2.18 | 3.61 | 0.0 | 0.0 |
| 22 | 4.36 | 3.61 | 0.0 | 0.0 |

TABLE 6. CONTACT PRESSURES, p , IN FOOTPRINT OF 49X17 (C-5B) TIRE
WITH 170 PSI INFLATION PRESSURE AND 39,600 POUND LOAD.

| Point | x (in) | y (in) | p (psi) | NCP |
|-------|--------|--------|---------|------|
| 1 | 0.0 | 0.0 | 68.6 | 0.40 |
| 2 | 3.06 | 0.0 | 66.0 | 0.39 |
| 3 | 6.12 | 0.0 | 70.6 | 0.41 |
| 4 | 9.19 | 0.0 | 44.4 | 0.26 |
| 5 | 12.25 | 0.0 | 0.0 | 0.0 |
| 6 | 0.0 | 0.70 | 229.6 | 1.35 |
| 7 | 3.06 | 0.70 | 219.6 | 1.29 |
| 8 | 6.12 | 0.70 | 217.5 | 1.28 |
| 9 | 9.19 | 0.70 | 140.3 | 0.83 |
| 10 | 12.25 | 0.70 | 0.0 | 0.0 |
| 11 | 0.0 | 2.10 | 244.2 | 1.44 |
| 12 | 3.03 | 2.10 | 233.2 | 1.37 |
| 13 | 6.06 | 2.10 | 233.3 | 1.37 |
| 14 | 9.09 | 2.10 | 153.1 | 0.90 |
| 15 | 12.12 | 2.10 | 0.0 | 0.0 |
| 16 | 0.0 | 3.51 | 241.7 | 1.42 |
| 17 | 2.97 | 3.51 | 224.5 | 1.32 |
| 18 | 5.94 | 3.51 | 245.4 | 1.44 |
| 19 | 8.90 | 3.51 | 3.6 | 0.02 |
| 20 | 11.88 | 3.51 | 0.0 | 0.0 |
| 21 | 0.0 | 4.23 | 323.9 | 1.91 |
| 22 | 2.92 | 4.23 | 326.0 | 1.92 |
| 23 | 5.85 | 4.23 | 282.0 | 1.66 |
| 24 | 8.77 | 4.23 | 0.0 | 0.0 |
| 25 | 0.0 | 5.00 | 275.3 | 1.62 |
| 26 | 2.87 | 5.00 | 201.3 | 1.18 |
| 27 | 5.74 | 5.00 | 0.0 | 0.0 |
| 28 | 0.0 | 5.72 | 0.0 | 0.0 |
| 29 | 2.80 | 5.72 | 0.0 | 0.0 |

TABLE 7. CONTACT PRESSURES, p , IN FOOTPRINT OF 20.00-20 (C-130E) TIRE
WITH 125 PSI INFLATION PRESSURE AND 46,500 POUND LOAD.

| Point | x (in) | y (in) | p (psi) | NCP |
|-------|--------|--------|---------|------|
| 1 | 0.0 | 0.0 | 74.2 | 0.59 |
| 2 | 3.52 | 0.0 | 223.1 | 1.78 |
| 3 | 7.03 | 0.0 | 65.1 | 0.52 |
| 4 | 10.55 | 0.0 | 66.2 | 0.53 |
| 5 | 14.07 | 0.0 | 0.0 | 0.0 |
| 6 | 0.0 | 0.70 | 150.3 | 1.20 |
| 7 | 3.51 | 0.70 | 148.1 | 1.18 |
| 8 | 7.03 | 0.70 | 136.5 | 1.09 |
| 9 | 10.54 | 0.70 | 107.5 | 0.86 |
| 10 | 14.05 | 0.70 | 0.0 | 0.0 |
| 11 | 0.0 | 1.40 | 167.9 | 1.34 |
| 12 | 3.50 | 1.40 | 166.3 | 1.33 |
| 13 | 7.01 | 1.40 | 158.3 | 1.27 |
| 14 | 10.51 | 1.40 | 128.7 | 1.03 |
| 15 | 14.02 | 1.40 | 0.0 | 0.0 |
| 16 | 0.0 | 2.10 | 177.3 | 1.42 |
| 17 | 3.49 | 2.10 | 171.1 | 1.37 |
| 18 | 6.98 | 2.10 | 161.5 | 1.29 |
| 19 | 10.46 | 2.10 | 122.7 | 0.98 |
| 20 | 13.95 | 2.10 | 0.0 | 0.0 |
| 21 | 0.0 | 3.50 | 203.6 | 1.63 |
| 22 | 3.44 | 3.50 | 197.3 | 1.58 |
| 23 | 6.87 | 3.50 | 193.3 | 1.55 |
| 24 | 10.31 | 3.50 | 133.3 | 1.07 |
| 25 | 13.74 | 3.50 | 0.0 | 0.0 |
| 26 | 0.0 | 4.21 | 192.1 | 1.54 |
| 27 | 3.40 | 4.21 | 179.5 | 1.44 |
| 28 | 6.79 | 4.21 | 169.5 | 1.36 |
| 29 | 10.19 | 4.21 | 0.0 | 0.0 |
| 30 | 0.0 | 4.93 | 237.5 | 1.90 |
| 31 | 3.35 | 4.93 | 210.8 | 1.69 |
| 32 | 6.70 | 4.93 | 302.2 | 2.42 |
| 33 | 10.06 | 4.93 | 0.0 | 0.0 |

TABLE 7. CONTACT PRESSURES, p , IN FOOTPRINT OF 20.00-20 (C-130E) TIRE
WITH 125 PSI INFLATION PRESSURE AND 46,500 POUND LOAD
(CONCLUDED).

| Point | x (in) | y (in) | p (psi) | NCP |
|-------|--------|--------|---------|------|
| 34 | 0.0 | 5.68 | 321.4 | 2.57 |
| 35 | 3.30 | 5.68 | 373.4 | 2.99 |
| 36 | 6.60 | 5.68 | 61.6 | 0.49 |
| 37 | 9.89 | 5.68 | 0.0 | 0.0 |
| 38 | 0.0 | 6.47 | 229.3 | 1.83 |
| 39 | 3.23 | 6.47 | 66.9 | 0.54 |
| 40 | 6.47 | 6.47 | 0.0 | 0.0 |
| 41 | 0.0 | 7.16 | 0.0 | 0.0 |
| 42 | 3.17 | 7.16 | 0.0 | 0.0 |

TABLE 8. CONTACT PRESSURES, p , IN FOOTPRINT OF B46X16.0-23.5 (B-1B)
TIRE WITH 260 PSI INFLATION PRESSURE AND 53,800 POUND LOAD.

| Point | x (in) | y (in) | p (psi) | NCP |
|-------|--------|--------|---------|------|
| 1 | 0.0 | 0.0 | 143.2 | 0.55 |
| 2 | 2.30 | 0.0 | 665.7 | 2.56 |
| 3 | 4.61 | 0.0 | 459.1 | 1.76 |
| 4 | 6.91 | 0.0 | 80.2 | 0.31 |
| 5 | 9.22 | 0.0 | 0.0 | 0.0 |
| 6 | 0.0 | 0.60 | 363.1 | 1.40 |
| 7 | 2.30 | 0.60 | 325.9 | 1.25 |
| 8 | 4.61 | 0.60 | 383.3 | 1.47 |
| 9 | 6.91 | 0.60 | 164.4 | 0.63 |
| 10 | 9.22 | 0.60 | 0.0 | 0.0 |
| 11 | 0.0 | 1.20 | 361.2 | 1.39 |
| 12 | 2.30 | 1.20 | 314.5 | 1.21 |
| 13 | 4.61 | 1.20 | 377.3 | 1.45 |
| 14 | 6.91 | 1.20 | 150.6 | 0.58 |
| 15 | 9.22 | 1.20 | 0.0 | 0.0 |
| 16 | 0.0 | 1.80 | 375.2 | 1.44 |
| 17 | 2.29 | 1.80 | 323.9 | 1.25 |
| 18 | 4.58 | 1.80 | 389.2 | 1.50 |
| 19 | 6.88 | 1.80 | 157.9 | 0.61 |
| 20 | 9.17 | 1.80 | 0.0 | 0.0 |
| 21 | 0.0 | 2.40 | 324.5 | 1.25 |
| 22 | 2.28 | 2.40 | 270.3 | 1.04 |
| 23 | 4.57 | 2.40 | 350.4 | 1.35 |
| 24 | 6.85 | 2.40 | 81.2 | 0.31 |
| 25 | 9.13 | 2.40 | 0.0 | 0.0 |
| 26 | 0.0 | 3.00 | 340.7 | 1.31 |
| 27 | 2.27 | 3.00 | 291.7 | 1.12 |
| 28 | 4.54 | 3.00 | 335.5 | 1.29 |
| 29 | 6.81 | 3.00 | 155.0 | 0.60 |
| 30 | 9.08 | 3.00 | 0.0 | 0.0 |
| 31 | 0.0 | 3.60 | 424.2 | 1.63 |
| 32 | 2.25 | 3.60 | 344.7 | 1.33 |
| 33 | 4.51 | 3.60 | 491.2 | 1.89 |
| 34 | 6.76 | 3.60 | 55.3 | 0.21 |
| 35 | 9.02 | 3.60 | 0.0 | 0.0 |

TABLE 8. CONTACT PRESSURES, p , IN FOOTPRINT OF B46X16.0-23.5 (B-1B) TIRE WITH 260 PSI INFLATION PRESSURE AND 53,800 POUND LOAD (CONCLUDED).

| Point | x (in) | y (in) | p (psi) | NCP |
|-------|--------|--------|---------|------|
| 36 | 0.0 | 4.81 | 452.3 | 1.74 |
| 37 | 2.20 | 4.81 | 465.7 | 1.79 |
| 38 | 4.41 | 4.81 | 446.4 | 1.72 |
| 39 | 6.61 | 4.81 | 0.0 | 0.0 |
| 40 | 0.0 | 5.98 | 497.5 | 1.91 |
| 41 | 2.13 | 5.98 | 343.1 | 1.32 |
| 42 | 4.27 | 5.98 | 0.0 | 0.0 |
| 43 | 0.0 | 6.55 | 0.0 | 0.0 |
| 44 | 2.09 | 6.55 | 0.0 | 0.0 |

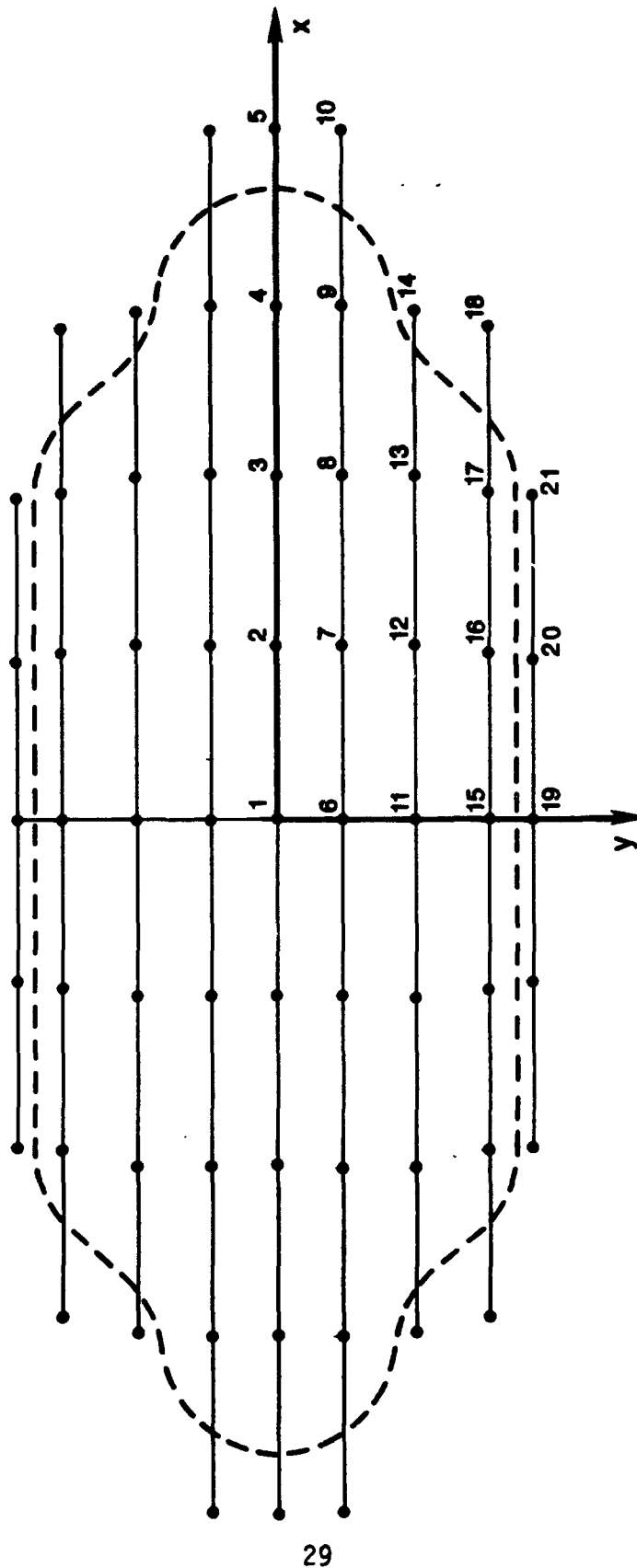


Figure 15. Calculated Pressure Locations in Footprint of T-38 Tire, Full-Scale.

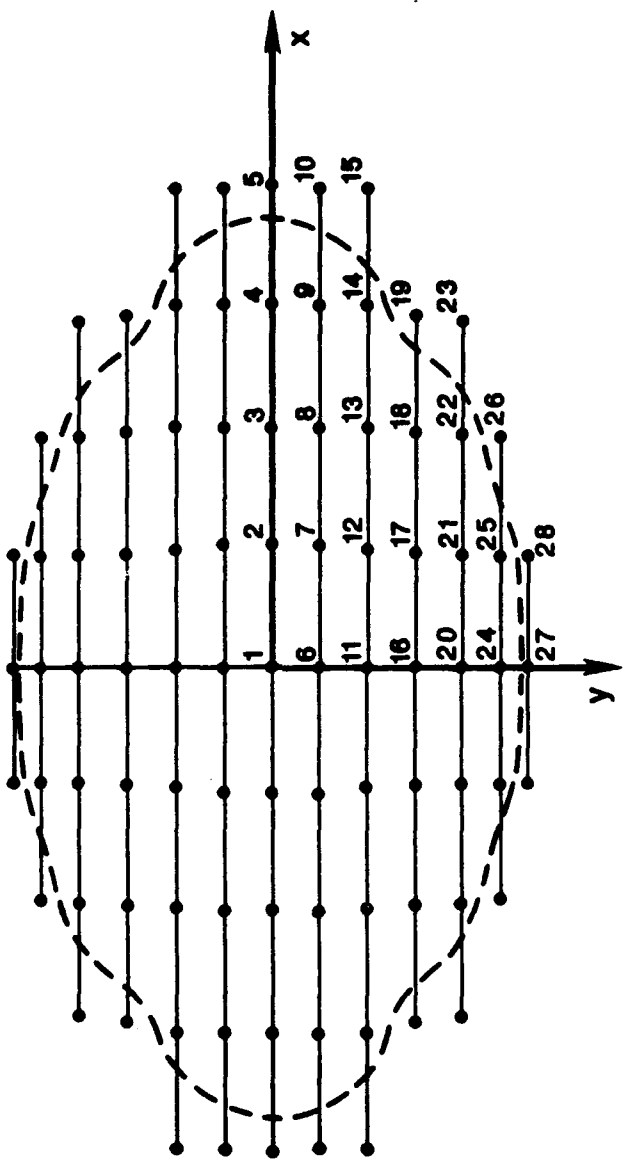


Figure 16. Calculated Pressure Locations in Footprint of F-16 Tire, Half-Scale.

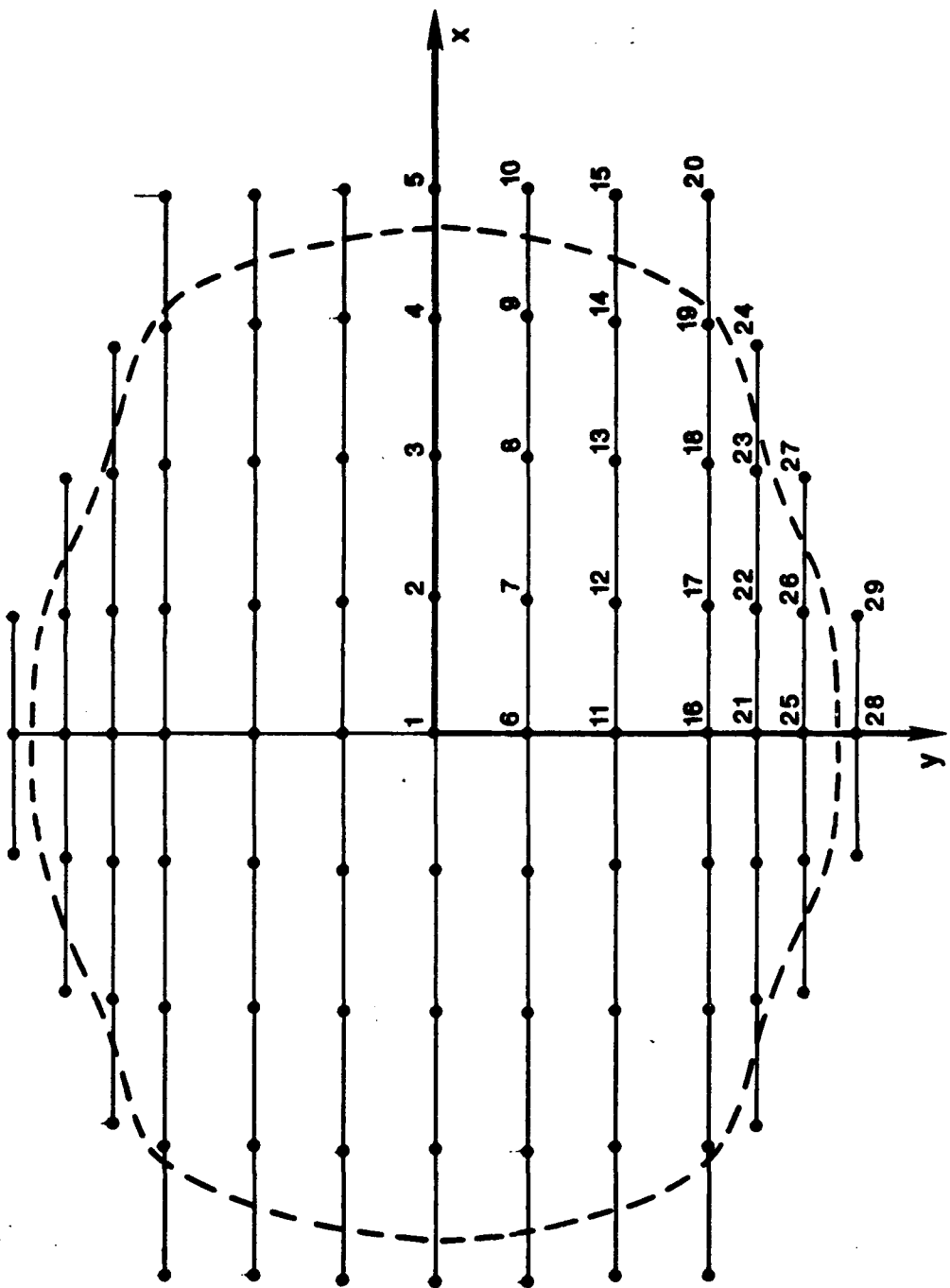


Figure 17. Calculated Pressure Locations in Footprint of F-4C/G Tire, Half-Scale.

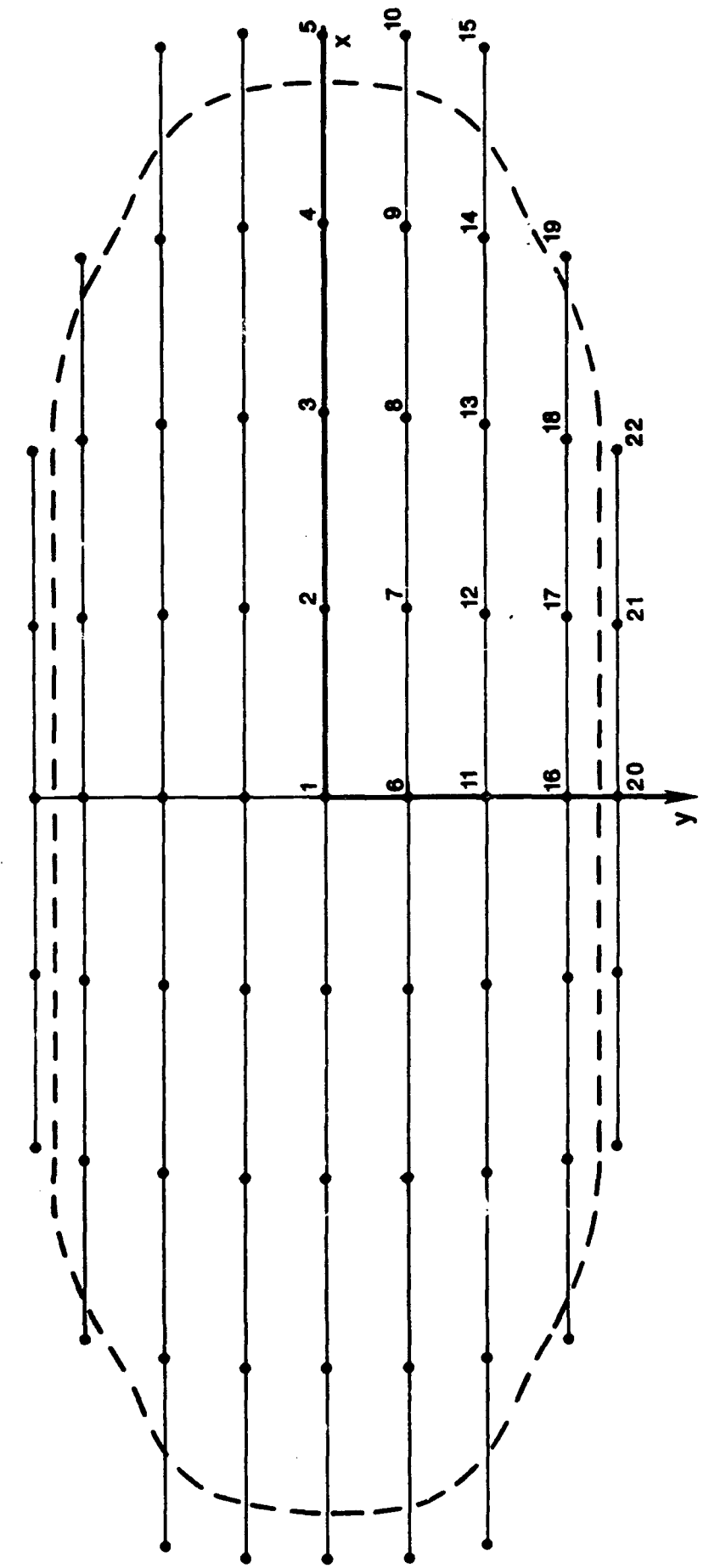


Figure 18. Calculated Pressure Locations in Footprint of F-15E Tire, Half-Scale.

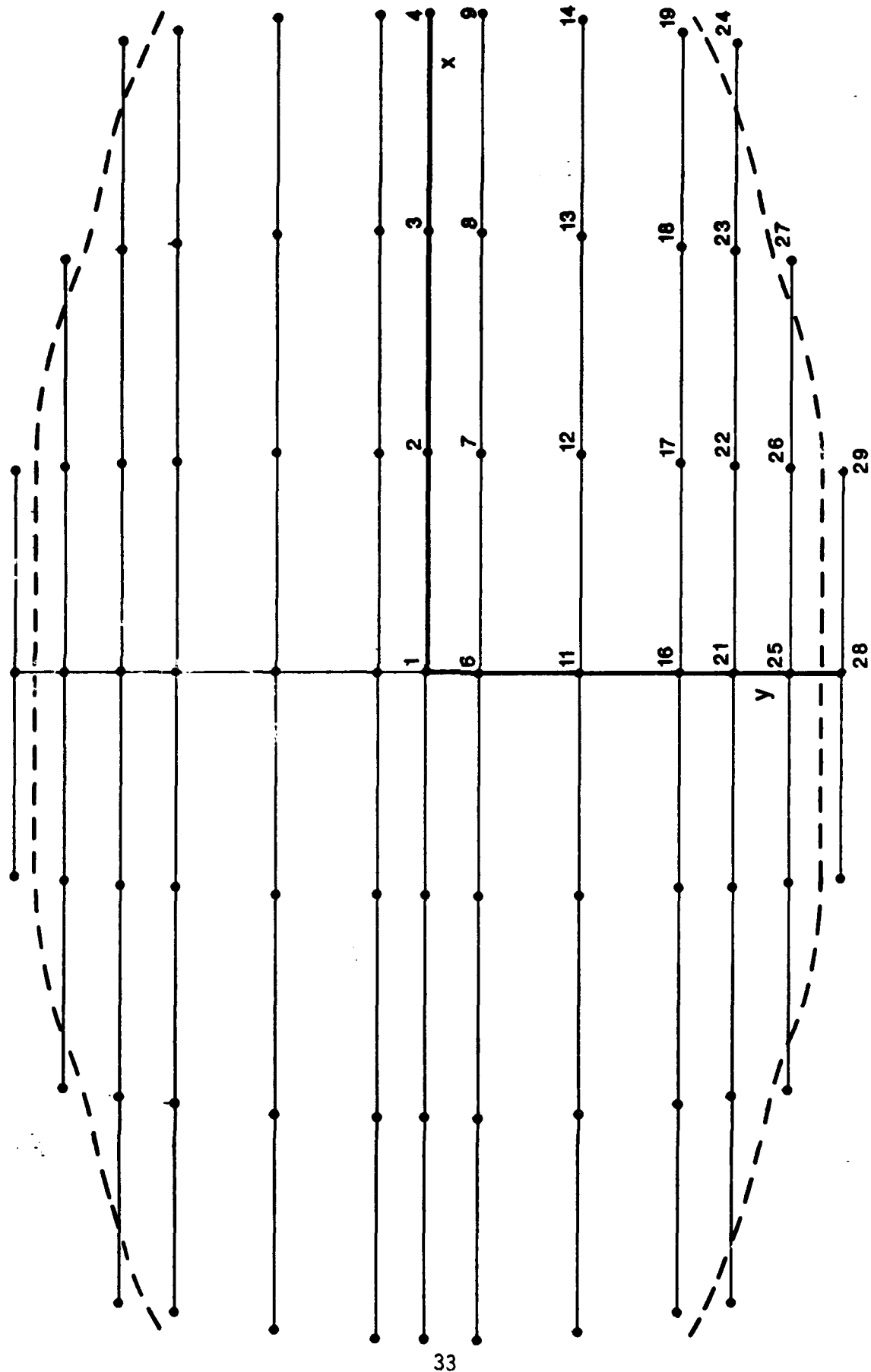


Figure 19. Calculated Pressure Locations in Footprint of C-5B Tire, Half-Scale.

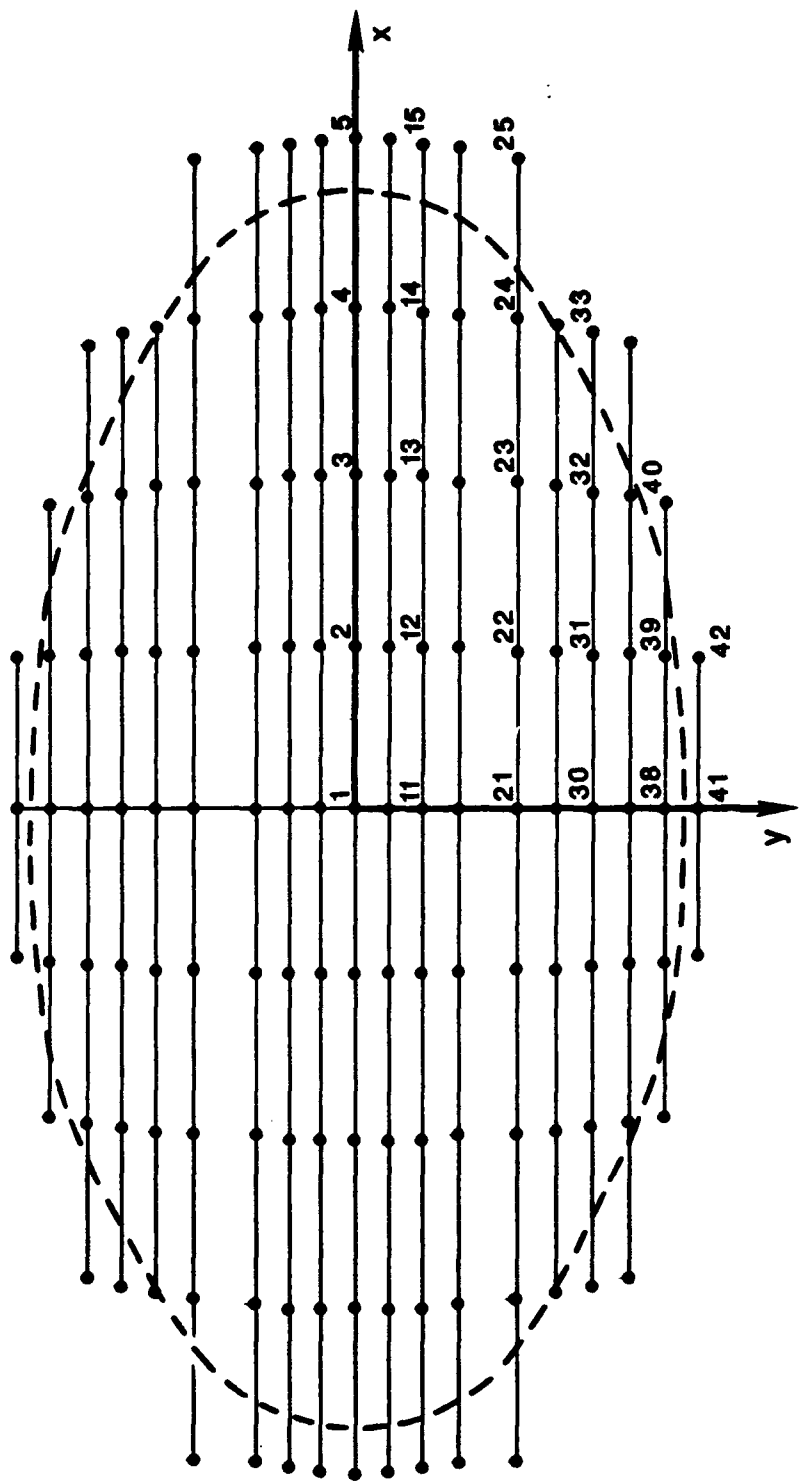


Figure 20. Calculated Pressure Locations in Footprint of C-130E Tire, Quarter-Scale.

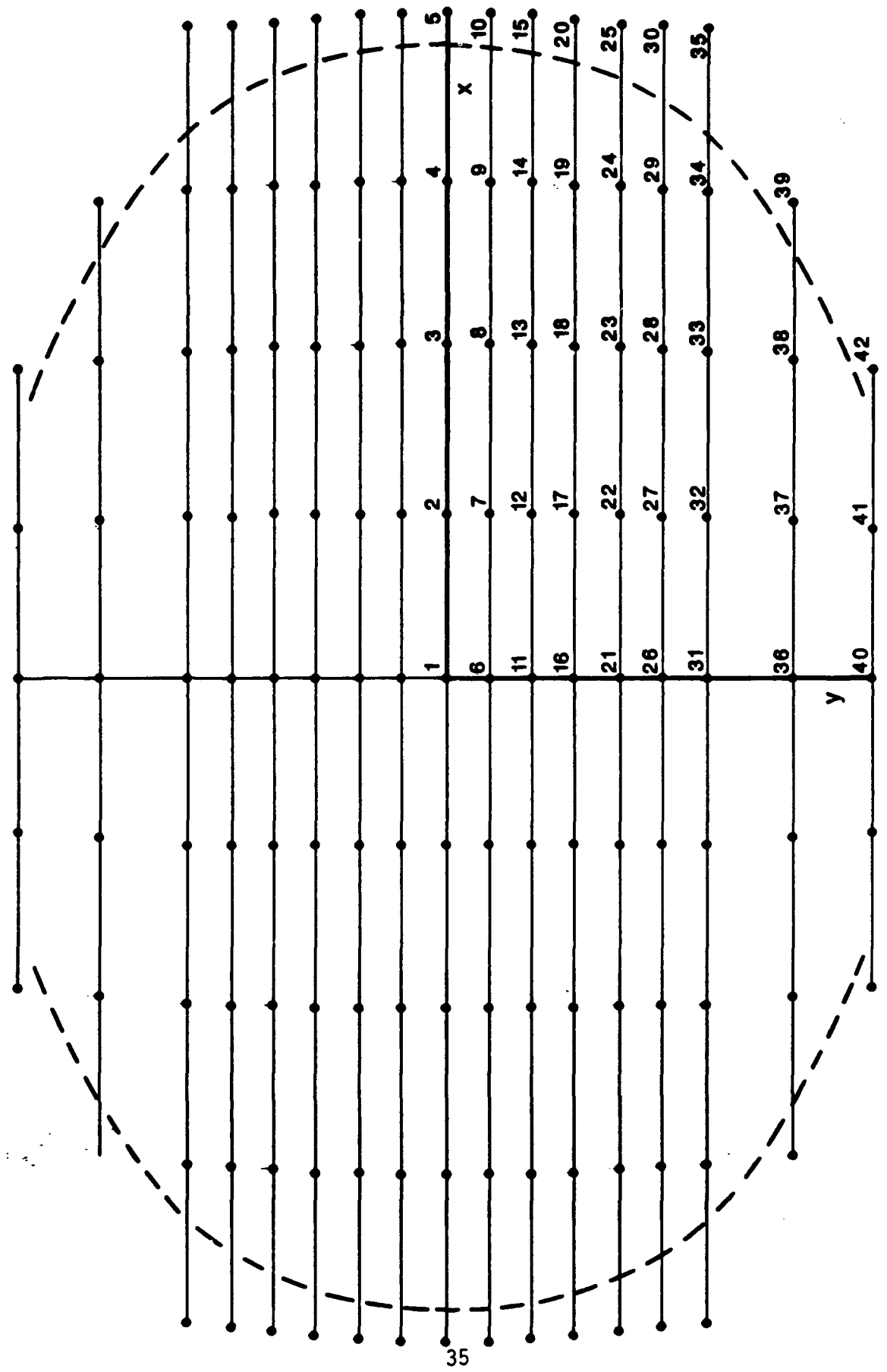


Figure 21. Calculated Pressure Locations in Footprint of 8-18 Tire, Half-Scale.

zero pressure points are included in the tables so that the footprint boundary can be approximately located, as shown by the dashed curve in Figure 15.

The contact pressures are not calculated on a rectangular grid in the footprint because finite elements of unequal length are used to model the tire and the point spacing along a finite element node depends on the radius of the node. The nodes in the tire footprint are parallel to the x-axis; pressure points are equally spaced along an individual node.

D. EFFECT OF INFLATION PRESSURE AND TIRE LOAD

The 3-D plots shown in Figures 22-25 were made to show the influence of inflation pressure and load on the pavement pressure distribution. These plots are all of pressures produced by the F-4C/G tire, and should be compared with Figure 3 which shows the pressure distribution for this tire at the rated inflation pressure and rated load.

Figures 22 and 23 show the distributions obtained at rated inflation pressure and loads that are 25 percent above and 25 percent below the rated load. In both cases, a more nonuniform pressure distribution was obtained, compared with that seen in Figure 3. Figures 24 and 25 show the effect of increasing or reducing the inflation pressure by 15 percent while holding the load fixed at the rated value. In these cases, also, more nonuniform pressure distributions were found. It appears, for the F-4 tire modeled here, that the most uniform tire/pavement pressure distribution is developed when the tire is operated at its rated inflation pressure and rated load. Ability to operate with as uniform a pavement pressure as possible is one of the goals of tire design.

Normalized contact pressure - F-4 tire
(33250 LB LOAD, 265 PSI INFLATION)
(NORMALIZED TO INFLATION PRESSURE)

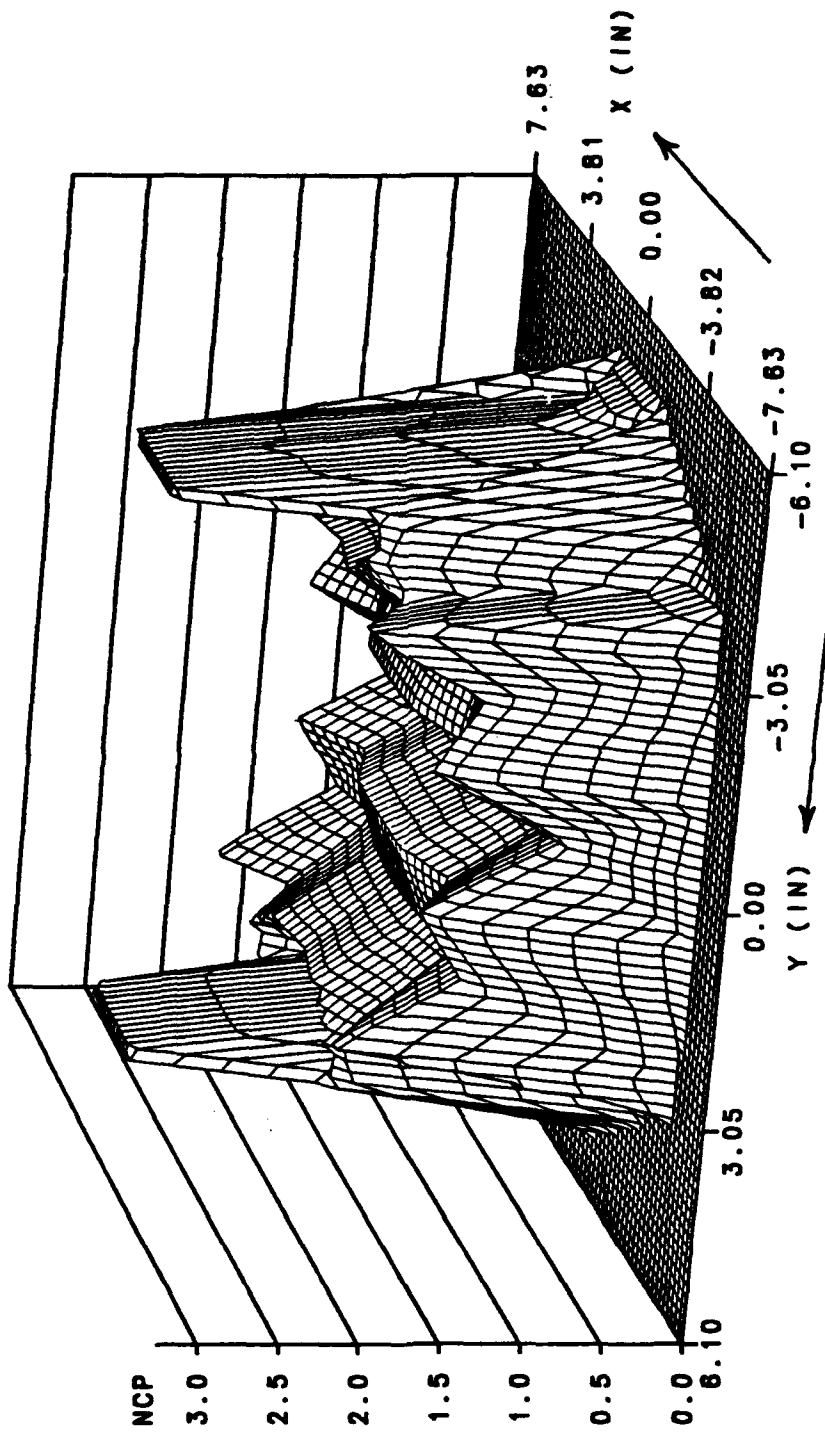


**Figure 22. Pavement Pressure Distribution Produced by the F-4C/G Tire
at Rated Inflation Pressure and 25 Percent Overload.**

Normalized contact pressure - F-4 tire
(19950 LB LOAD, 265 PSI INFLATION)
(NORMALIZED TO INFLATION PRESSURE)

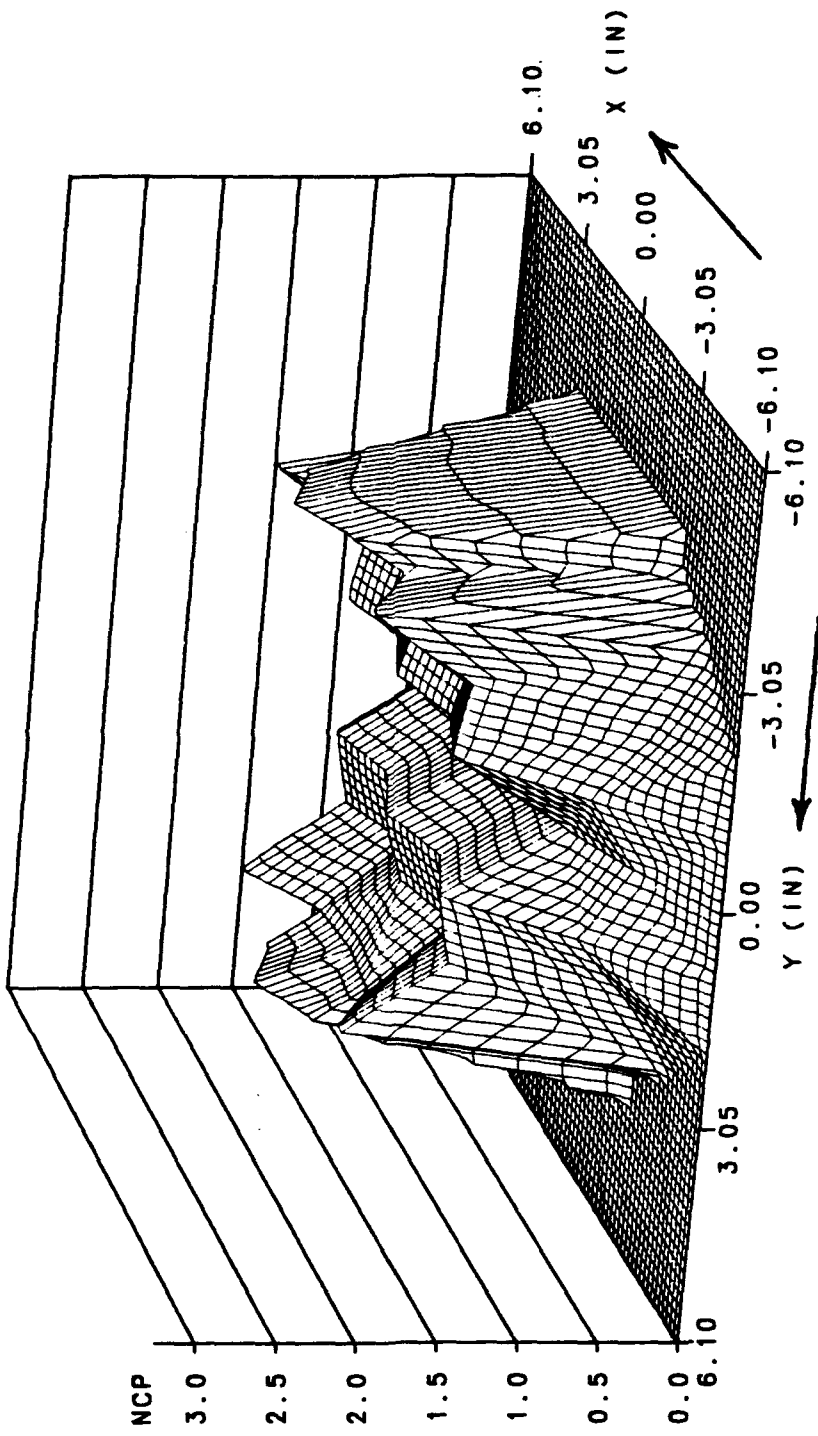


Figure 23. Pavement Pressure Distribution Produced by the F-4C/G Tire at Rated Inflation Pressure and 25 Percent Underload.

Normalized contact pressure - F-4 tire
(26600 LB LOAD, 305 PSI INFLATION)
(NORMALIZED TO INFLATION PRESSURE)

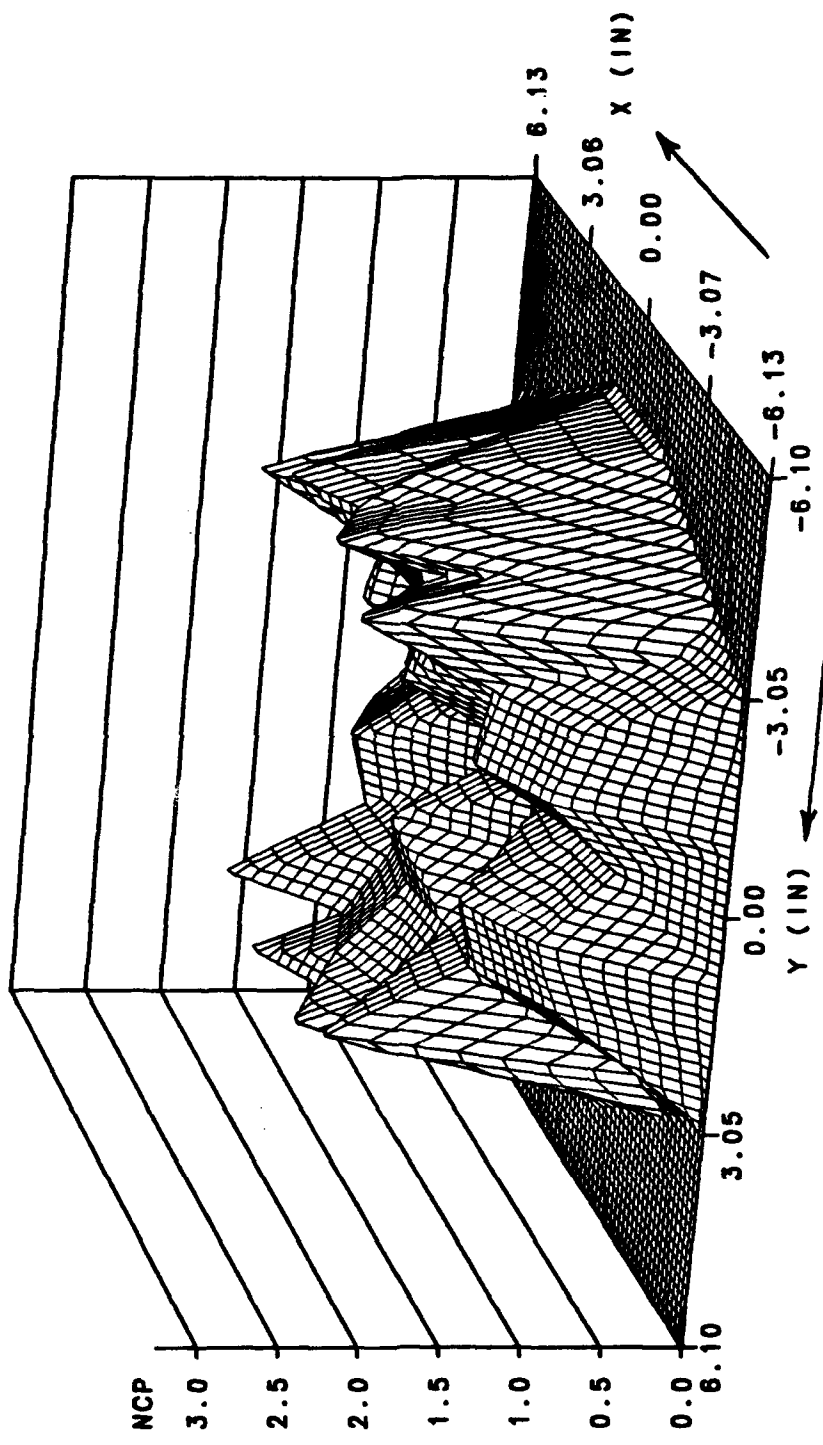
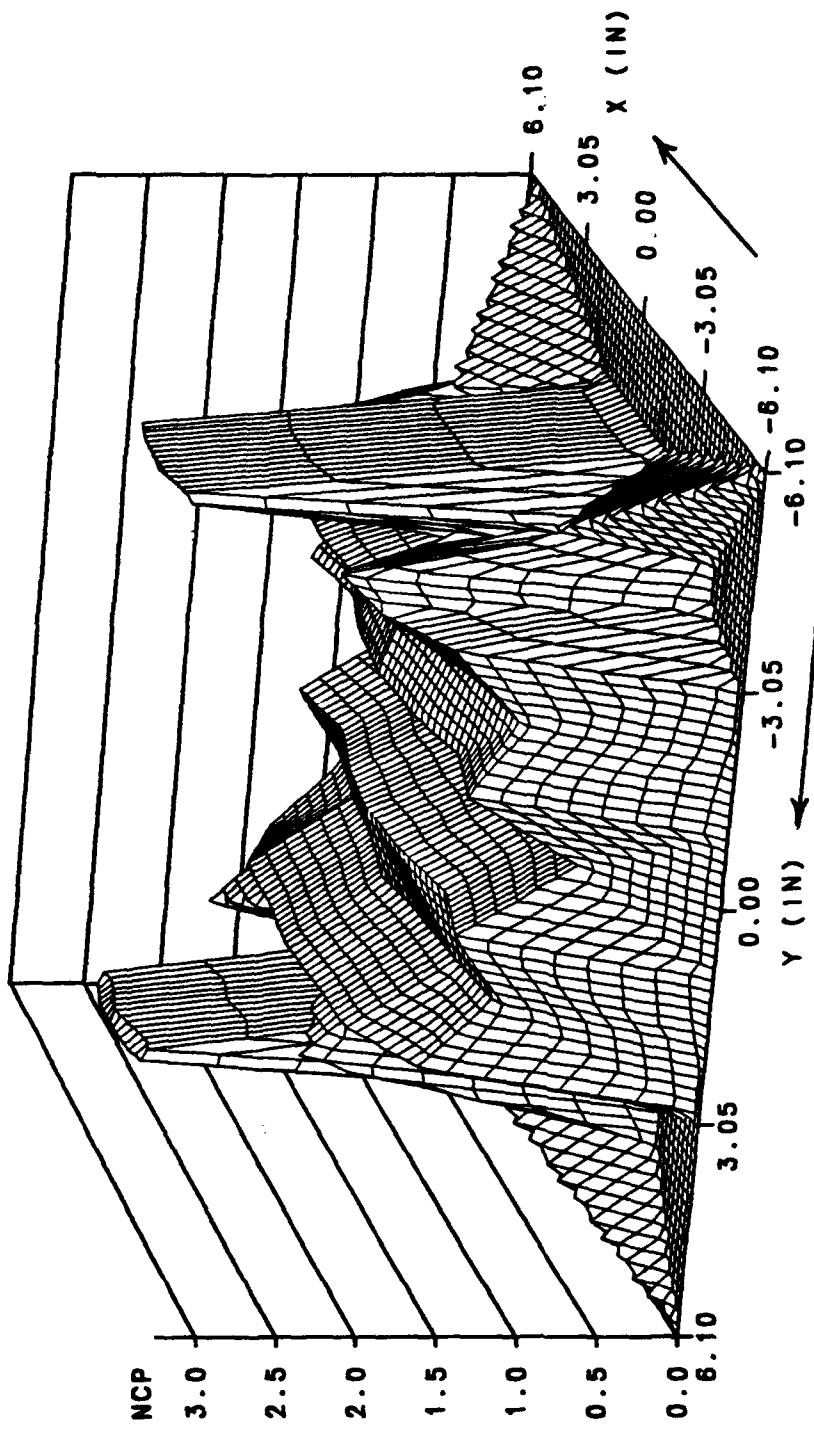


Figure 24. Pavement Pressure Distribution Produced by the F-4C/G Tire
at 15 Percent Overpressure and Rated Load.

Normalized contact pressure - F-4 tire
(26600 LB LOAD, 25 PSI INFLATION)
(NORMALIZED TO INFLATION PRESSURE)



**Figure 25. Pavement Pressure Distribution Produced by the F-4C/G Tire
at 15 Percent Underpressure and Rated Load.**

SECTION III

CONCLUSIONS AND RECOMMENDATIONS

A. CONCLUSIONS

The calculated results shown in the previous section represent contact pressures for a standing tire, deflected against a frictionless surface. Studies of passenger car tires (Reference 4) show that surface friction has little effect on the pavement pressure developed by a standing or freely-rolling tire. Centrifugal force stiffening occurs in a rolling tire, but the effect on pavement pressure is negligible except at extremely high speeds. The conjecture may be made that pavement pressure of a taxiing airplane will be essentially the same as the pavement pressure when the plane is parked, regardless of the nature of the pavement surface.

The calculated pavement pressure distributions shown in this report should be regarded as approximate, because of the many engineering approximations embodied in the tire model. However, the calculated distributions are sensitive to basic tire design parameters and also to tire operating variables (inflation pressure and load). They appear to be qualitatively correct.

Although rudimentary and empirical tire models can reproduce tire deflection-load data much closer than the tire model here does (Figure 8-14), these models are incapable of calculating a tire/pavement pressure distribution.

Tire stiffness is primarily responsible for nonuniformity in the pavement pressure distribution. The distributions found here are all characterized by reduced pressure along the central portion of the tread, and highest pressure in the shoulder region (near the edges of the tread). Generally higher

inflation pressure results in a stiffer tire and a more nonuniform contact pressure. However, the effect can be mitigated by tire design. An example is seen in comparing the pressure distributions found for the F-16 (Figure 2) and the F-15E (Figure 4) tires. Although these tires operate at nearly the same inflation pressure, which is quite high, the distribution found for the F-15E tire is much more uniform than that found for the F-16 tire. The difference is, in large part, due to the F-16 tire being a bias-ply tire and the F-15E tire being a radial.

B. RECOMMENDATIONS

With continued development of pavement analysis tools, knowledge of the distribution of tire/pavement contact pressure may become as important for pavement design as knowledge of pavement material properties. Since pavement pressure distributions are quite sensitive to tire inflation pressure and tire load, a computer tire model such as that employed in this project should be made available to pavement engineers.

In view of the scarcity of measured aircraft tire/pavement pressure distributions it is recommended that the Air Force develop the capability to measure pavement pressure distributions. This is not a simple undertaking.

As the tire model used in this project has not been adequately validated, it would be desirable to measure contact pressures for some, or all, of the tires studied here. The pressure measurements should be made for both new and worn tires, as the effect of the tread layer on contact pressure is not well understood. The tire model used here ignores the tread layer entirely.

A standing tire contact pressure distribution (at rated inflation pressure and load) should be included in the Qualification Test Report (QTR), and additional tire data should be included in the QTR to make it and the accompanying tire section a complete source of tire data needed by whatever tire model is adopted by the Air Force.

REFERENCES

1. Hollaway, R., Aircraft Characteristics for Airfield Pavement Design and Evaluation, Air Force Engineering and Services Center, Tyndall AFB, Florida, May 1988.
2. Tielking, J.T., and Roberts, F.L., "Tire Contact Pressure and Its Effect on Pavement Strain," ASCE Journal of Transportation Engineering, Vol. 113, No. 1, pp. 56-71, 1987.
3. Tielking, J.T., "A Finite Element Tire Model," Tire Science and Technology, Vol. 11, Nos. 1-4, pp. 50-63, 1983.
4. Clark, S.K., Editor, Mechanics of Pneumatic Tires, DOT HAS 805 952, U.S. Department of Transportation, National Highway Traffic Safety Administration, Washington, D.C., August 1981.

APPENDIX A

TIRE DATA AND PROFILES

A. TIRE DATA

The finite element tire model used in this project requires input data describing the geometry of the tire section (meridian profile), the carcass structure, and material properties of the tire carcass constituents (cord and rubber). The mounted meridian profile of each of the tires in this project is shown in Figures A-1 through A-6, where the finite element model is the dotted curve shown in the left half of each profile. The tires are considered to have a plane of geometric symmetry for modeling purposes, so only one-half of the profile is modeled. Each dot in the finite element curve is a connection (node) between finite elements, of which the Cartesian coordinates and slope are input to the computer program. This describes the tire's basic geometry in the mounted, uninflated configuration.

Another section of tire model input data describes the structure of, and material properties in, the tire carcass. The following carcass data are needed:

- (1) Ply Count and Thickness of Each Ply
- (2) Cord Diameter (in each ply)
- (3) Cord End Count (in each ply, at each finite element node)
- (4) Cord Angle (wrt meridian, in each ply, at each node)
- (5) Cord Moduli
- (6) Rubber Moduli

As nylon 66 tire cord is used in all of the tires considered here, the cord extension modulus 200,000 psi was used for all calculations. The cord is treated as being transversely isotropic, with Poisson ratio 0.70 and shear modulus 700 psi. Rubber is considered to be isotropic with Young's modulus 1000 psi and Poisson ratio 0.493 for all of the tires.

Cord diameters vary with tire size, and may differ in different plies of the same tire. This information, together with end counts and angles, was provided upon special request to the tire manufacturers. Only the cord count in the crown is provided in the tire Qualification Test Report (item Q).

A physical section was obtained for each tire modeled. The section is used in laying out the meridian profile, locating carcass features such as turnups and belts (in the case of a radial tire), and measurement of ply thicknesses.

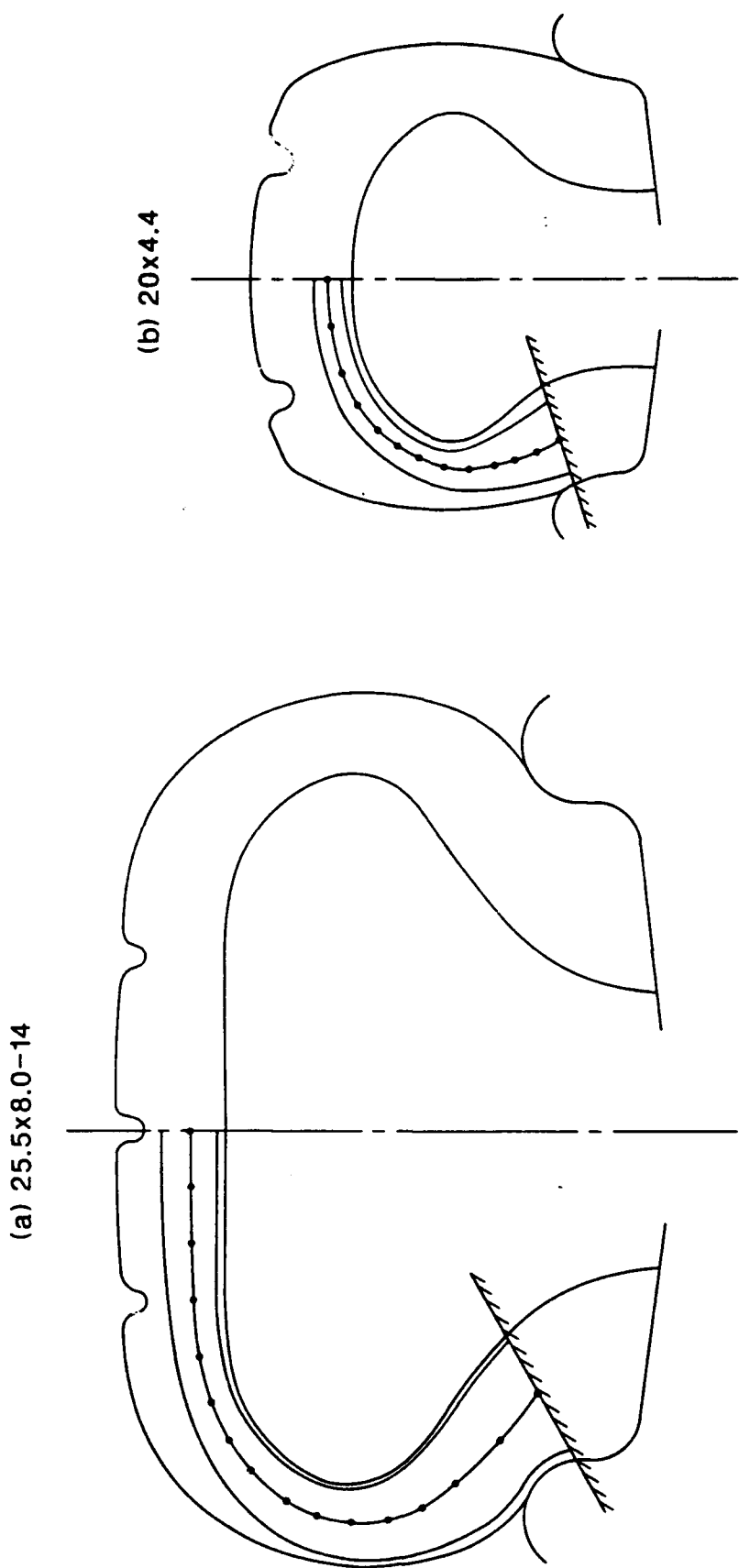


Figure A-1. Meridian Sections of
(a) 25.5x8.0-14 (F-16).
(b) 20x4x4 (T-38).
Both Full Size.

49

(The reverse of this page is blank)

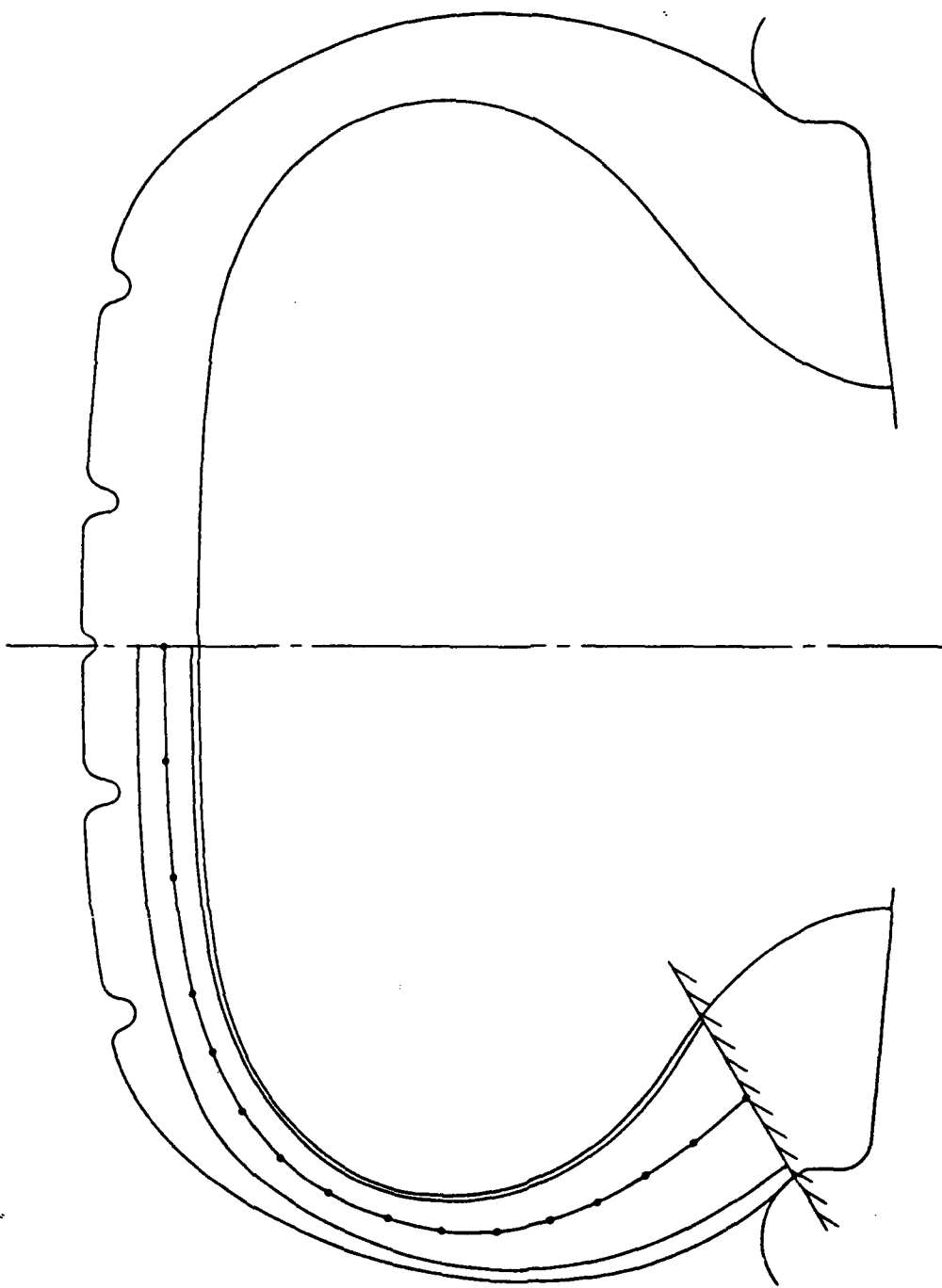


Figure A-2. Meridian Section of
30R11.5-14.5 (F-4C/G).
Full Size.

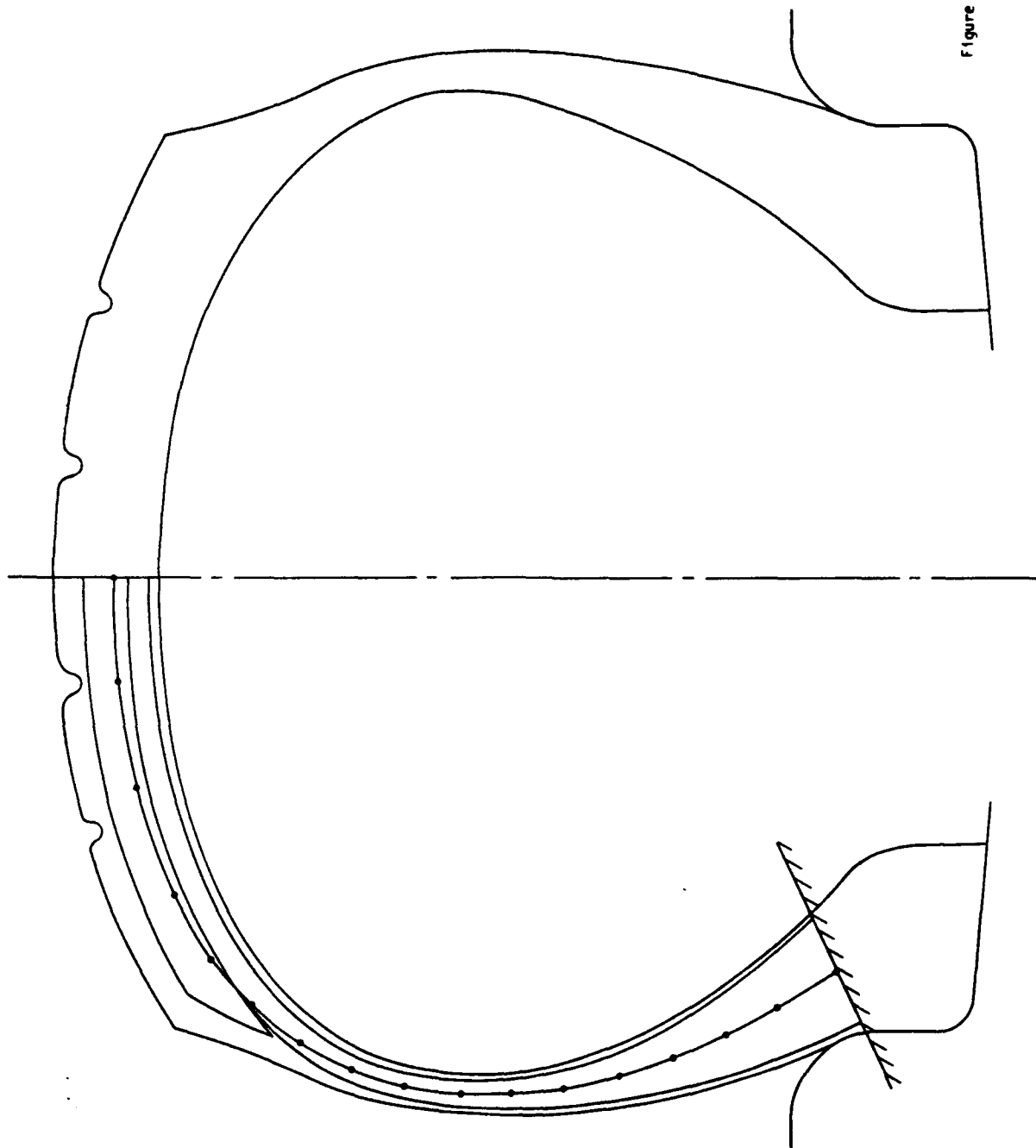


Figure A-3. Meridian Section of
36x18B (F-1SE).
Full Size.

53

(The reverse of this page is blank)

Figure A-4. Meridian Section of
49x17 (C-88).
Reduced 64 Percent.

55

(The reverse of this page is blank)

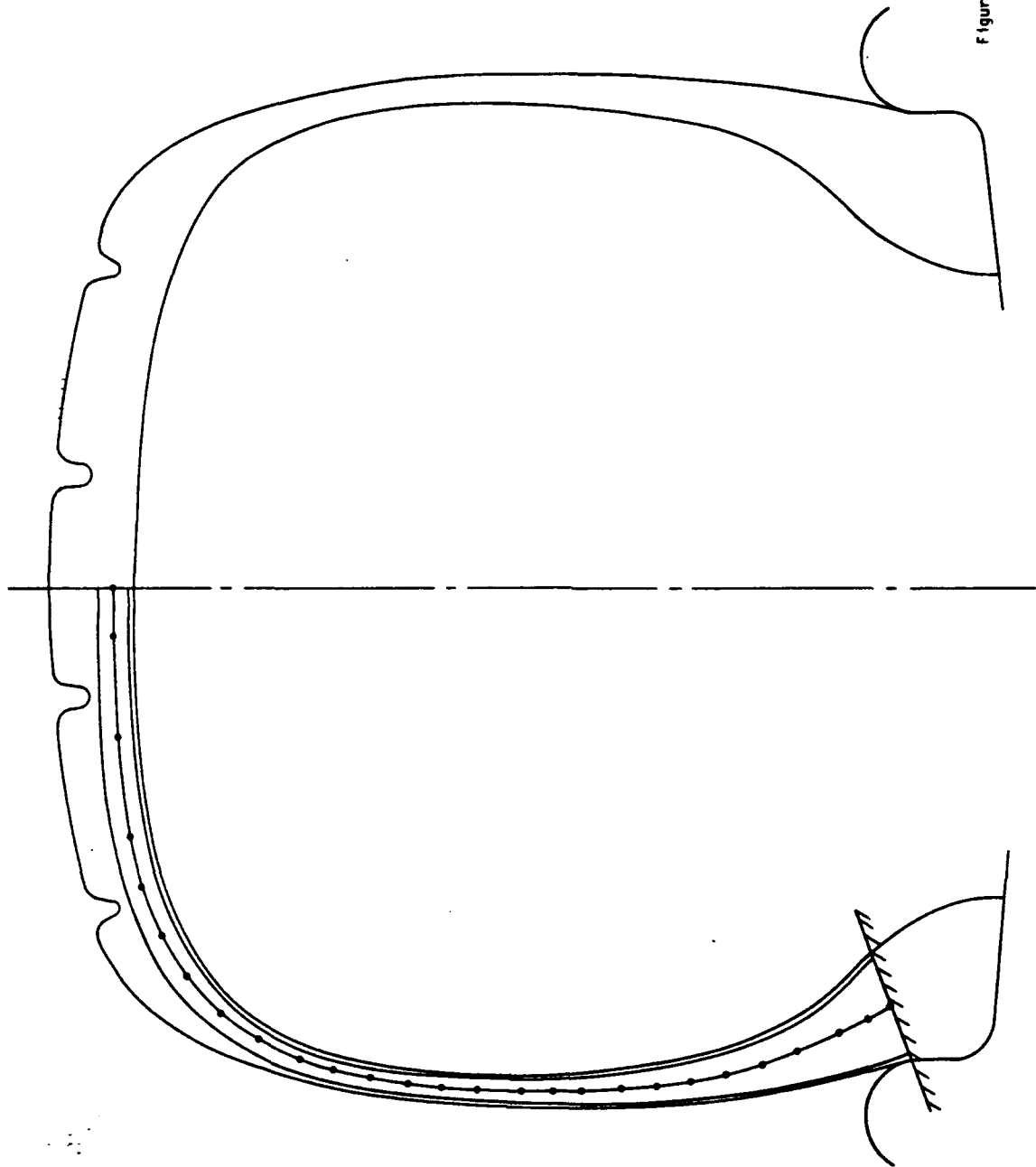
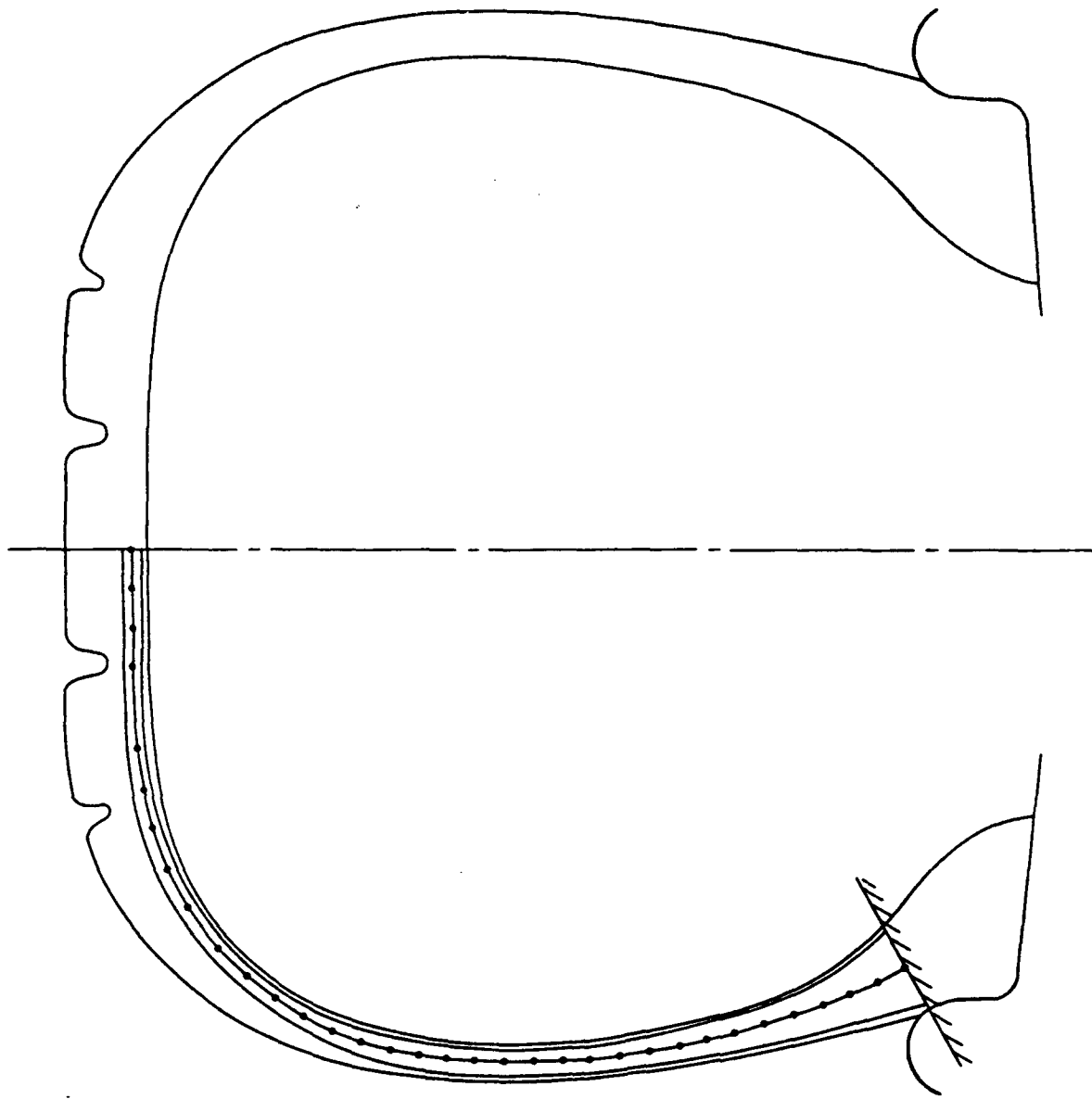


Figure A-5. Meridian Section of
20-00-20 (C-301),
Reduced 50 Percent.

§7

(The reverse of this page is blank)



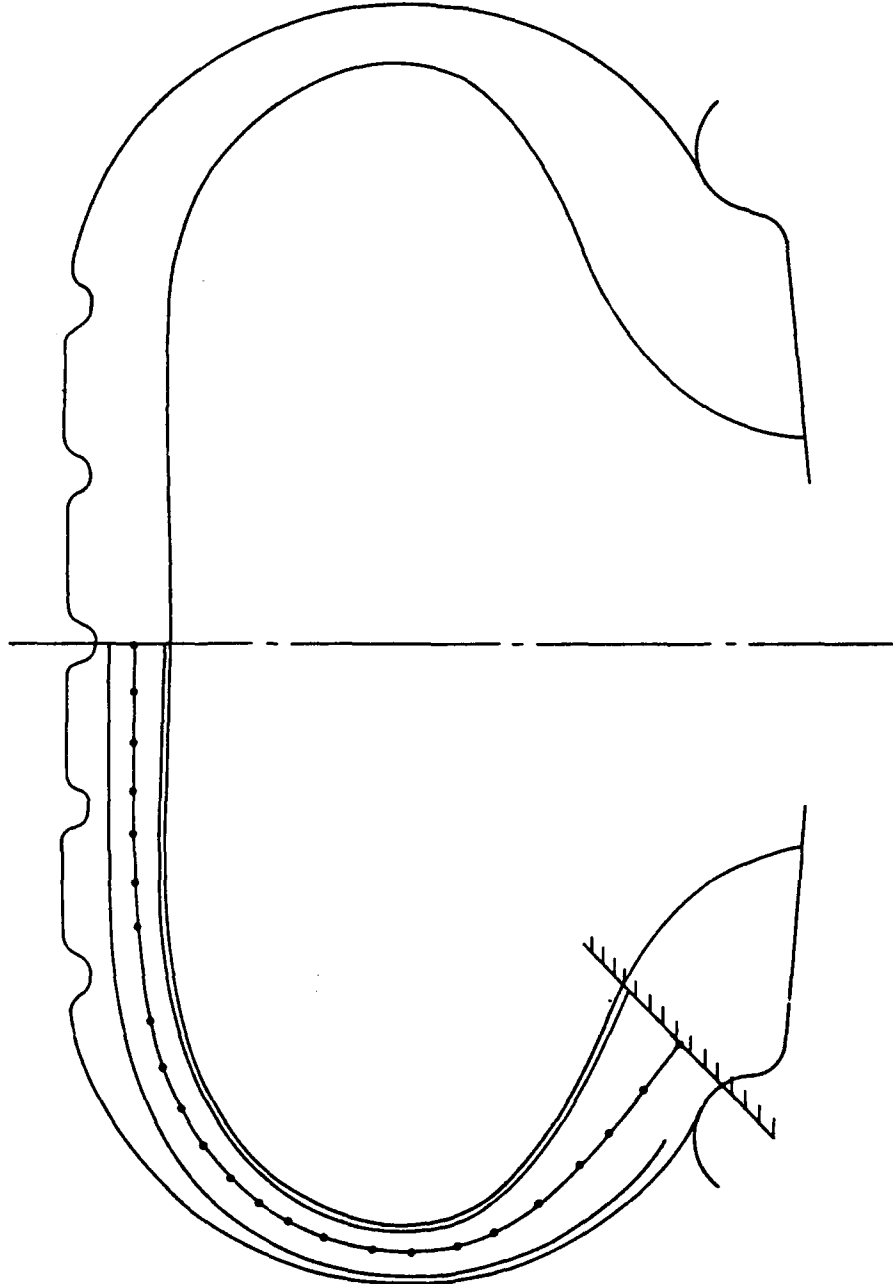


Figure A-6. Meridian Section of
B4616.0-23.5 (B-18).
Reduced 64 Percent.

59

(The reverse of this page is blank)